

Pulmonary macrophage transplantation therapy

Takuji Suzuki¹, Paritha Arumugam², Takuro Sakagami¹, Nico Lachmann³, Claudia Chalk¹, Anthony Salles¹, Shuichi Abe¹, Cole Trapnell^{4,5}, Brenna Carey¹, Thomas Moritz³, Punam Malik², Carolyn Lutzko², Robert E. Wood⁶ & Bruce C. Trapnell^{1,6,7}

Bone-marrow transplantation is an effective cell therapy but requires myeloablation, which increases infection risk and mortality. Recent lineage-tracing studies documenting that resident macrophage populations self-maintain independently of haematological progenitors prompted us to consider organ-targeted, cell-specific therapy. Here, using granulocyte-macrophage colony-stimulating factor (GM-CSF) receptor-β-deficient (*Csf2rb*^{-/-}) mice that develop a myeloid cell disorder identical to hereditary pulmonary alveolar proteinosis (hPAP) in children with CSF2RA or CSF2RB mutations, we show that pulmonary macrophage transplantation (PMT) of either wild-type or *Csf2rb*-gene-corrected macrophages without myeloablation was safe and well-tolerated and that one administration corrected the lung disease, secondary systemic manifestations and normalized disease-related biomarkers, and prevented disease-specific mortality. PMT-derived alveolar macrophages persisted for at least one year as did therapeutic effects. Our findings identify mechanisms regulating alveolar macrophage population size in health and disease, indicate that GM-CSF is required for phenotypic determination of alveolar macrophages, and support translation of PMT as the first specific therapy for children with hPAP.

Mutations in *CSF2RA* or *CSF2RB*, encoding GM-CSF receptor α or β, respectively, cause hPAP by impairing GM-CSF-dependent surfactant clearance by alveolar macrophages, resulting in progressive surfactant accumulation in alveoli and hypoxaemic respiratory failure^{1–5}. Surfactant normally comprises a thin phospholipid/protein layer reducing tension on the alveolar surface⁶ that is maintained by balanced secretion by alveolar type II epithelial cells and clearance by these cells and alveolar macrophages^{7,8}. PAP also occurs in people with GM-CSF autoantibodies (~85–90% of all patients with PAP)^{9,10} and mice with disruption of the GM-CSF gene *Csf2* (refs 11, 12) or the GM-CSF receptor β-subunit gene *Csf2rb* (refs 13, 14) (*Csf2*^{-/-} or *Csf2rb*^{-/-} mice, respectively). Characteristics of PAP caused by disruption of GM-CSF signalling include typical lung histopathology (well preserved alveoli filled with surfactant and ‘foamy’ macrophages staining positive with periodic acid-Schiff (PAS) or oil red O); turbid, ‘milky’ appearing bronchoalveolar lavage (BAL) caused by accumulated surfactant and cell debris; and a disease-specific pattern of biomarkers (increased GM-CSF (hPAP), M-CSF/CSF1 and MCP-1 in BAL fluid, and reduced mRNA for *PU.1*, *PPARG* and *ABCG1* in alveolar macrophages)^{1–5,15–20}.

Currently, no pharmacological therapy of hPAP exists and surfactant must be removed by whole-lung lavage, an inefficient, invasive procedure to physically remove excess surfactant^{2–4}. In *Csf2rb*^{-/-} mice, PAP was corrected by bone marrow transplantation (BMT) of wild-type (WT)²¹ or *Csf2rb*-gene-corrected *Csf2rb*^{-/-} haematopoietic stem/progenitor cells (HSPCs)²². However, in humans this approach resulted in death from infection before engraftment², probably as a result of required myeloablation/immunosuppressive therapy. Since pulmonary GM-CSF is increased in hPAP^{1–5} we hypothesized that macrophages administered directly into the lungs (pulmonary macrophage transplantation or PMT) without myeloablation would engraft and reverse the manifestations of hPAP.

We first validated *Csf2rb*^{-/-} mice as a model of human hPAP by demonstrating that they had the same clinical, physiological, histopathological

and biochemical abnormalities, disease biomarkers and natural history (Fig. 1 and Extended Data Fig. 1) as children with hPAP³.

Characterization of macrophages before PMT

Bone-marrow-derived macrophages (BMDMs) from WT mice had morphology and phenotypic markers (F4/80⁺, CD11b^{Hi}, CD11c⁺, CD14⁺, CD16/32⁺, CD64⁺, CD68⁺, CD115⁺, CD131⁺, SiglecF^{Low}, MerTK⁺, MHC class II⁺, Ly6G⁻, CD3⁻, CD19⁻) of macrophages (Extended Data Fig. 2a–c) and contained <0.0125% lineage negative (Lin⁻) Sca1⁺c-Kit⁺ (LSK) cells. Clonogenic analysis indicated <0.005% colony-forming units-granulocyte, monocyte/macrophage (CFU-GM) and no burst-forming units-erythrocyte (BFU-E) or colony-forming units-granulocyte, erythrocyte, monocyte/macrophage, megakaryocyte (CFU-GEMM) progenitors (Extended Data Fig. 2d, e). Functional evaluation²³ showed that the BMDMs could clear surfactant (Extended Data Fig. 2f, g). These results demonstrated that the cells used for PMT were highly purified, mature macrophages capable of surfactant clearance.

Efficacy of PMT of WT macrophages

To determine the therapeutic potential of PMT, *Csf2rb*^{-/-} mice received WT (*Csf2rb*^{+/+}) BMDMs by PMT once (Fig. 1a). One year later, PMT-derived CD131⁺ BAL cells were present (Fig. 1b), alveolar macrophages expressed *Csf2rb* (Extended Data Fig. 3a), and BAL was markedly improved with respect to opacification (Fig. 1c), sediment (Fig. 1c) and microscopic cytopathology (Extended Data Fig. 3b). Importantly, PMT nearly completely resolved the abnormal pulmonary histopathology (Fig. 1d and Extended Data Fig. 3c). Measurement of BAL turbidity and surfactant protein-D (SP-D) content (Fig. 1e), which reflect the extent of surfactant accumulation across the entire lung surface, confirmed the improvement in hPAP. BAL fluid biomarkers of hPAP were also improved (Fig. 1f). The effects of PMT were evident early, as demonstrated by detection of CD131⁺ alveolar macrophages with *Csf2rb* mRNA and protein (not

¹Division of Pulmonary Biology, Perinatal Institute, Cincinnati Children's Hospital Medical Center, 3333 Burnet Avenue, Cincinnati, Ohio 45229, USA. ²Division of Experimental Hematology, Cincinnati Children's Hospital Medical Center, 3333 Burnet Avenue, Cincinnati, Ohio 45229, USA. ³RG Reprogramming and Gene Therapy, Institute of Experimental Hematology, Hannover Medical School, Carl Neuberg-Str. 1, 30625 Hannover, Germany. ⁴Department of Stem Cell and Regenerative Biology, Harvard University, Cambridge, Massachusetts 02138, USA. ⁵Broad Institute of Massachusetts Institute of Technology and Harvard University, Cambridge, Massachusetts 02138, USA. ⁶Division of Pulmonary Medicine, Cincinnati Children's Hospital Medical Center, 3333 Burnet Avenue, Cincinnati, Ohio 45229, USA. ⁷Division of Pulmonary, Critical Care, and Sleep Medicine, University of Cincinnati Medical Center, 3333 Burnet Avenue, Cincinnati, Ohio 45229, USA.

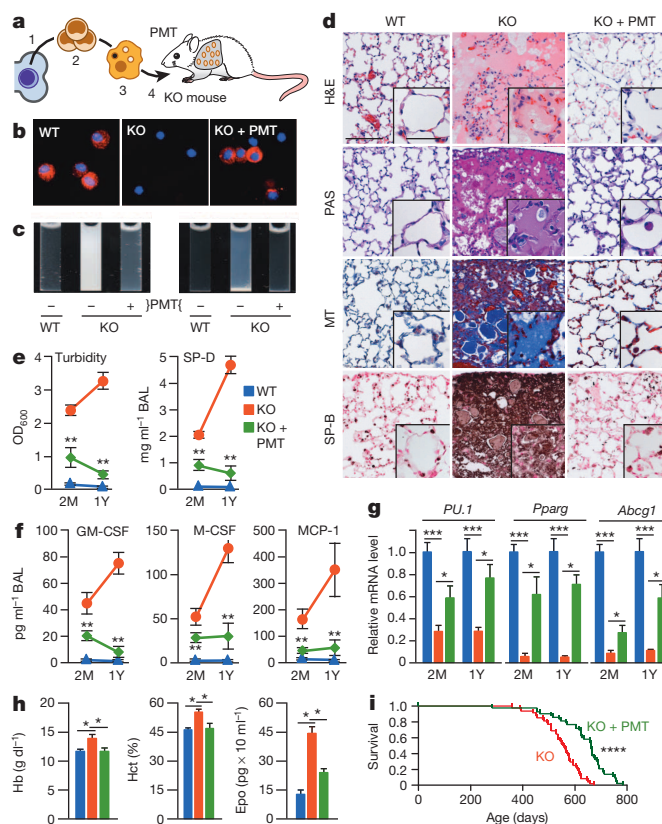


Figure 1 | Therapeutic efficacy of PMT in *Csf2rb*^{-/-} mice. **a**, Schematic of the method used. WT HSPCs (1) were isolated, expanded (2), differentiated into macrophages (3), and administered by endotracheal instillation into 2-month-old *Csf2rb*^{-/-} (KO) mice (4) and evaluated after 2 months (2M) (e–g) or one year (1Y) (b–h) with age-matched, untreated WT or *Csf2rb*^{-/-} mice (KO+PMT, WT or KO, respectively). **b**, CD131-immunostained BAL cells. **c**, Appearance of BAL fluid (left) or sediment (right). **d**, Lung histology after staining with haematoxylin and eosin (H&E), PAS, Masson's trichrome (MT), or surfactant protein B (SP-B). Scale bar, 100 µm; inset, 50 µm. **e**, BAL turbidity and SP-D concentration. **f**, BAL biomarkers. **g**, Alveolar macrophage biomarkers. **h**, Effects of PMT on blood haemoglobin (Hb), haematocrit (Hct) and serum erythropoietin (Epo). **i**, Kaplan-Meier analysis of PMT-treated ($n = 43$) and untreated *Csf2rb*^{-/-} mice ($n = 48$). Images are representative of 6 mice per group (b–d). Numeric data are mean \pm s.e.m. of 7 (2M) or 6 (1Y) mice per group. * $P < 0.05$, ** $P < 0.01$, *** $P < 0.001$, **** $P < 0.0001$.

shown), reduced BAL opacification and cytopathology (not shown), BAL turbidity (Fig. 1e), SP-D (Fig. 1e) and BAL fluid biomarkers (Fig. 1f) 2 months after PMT, and reduced lung histopathology 4 months after PMT (not shown). In contrast, PMT of *Csf2rb*^{-/-} BMDMs had no effect on BAL turbidity, SP-D content, or BAL fluid biomarkers (not shown), demonstrating that GM-CSF receptors on transplanted macrophages are important for the therapeutic effects.

To evaluate the effects of PMT on the alveolar macrophage population, we measured cellular biomarkers after PMT. Results showed that alveolar macrophages from PMT-treated *Csf2rb*^{-/-} mice had increased mRNA for *PU.1*, *Pparg* and *Abcg1*, improvement was significant by 2 months, and the effects persisted 1 year after PMT (Fig. 1g).

Since *Csf2rb*^{-/-} mice develop polycythaemia, a secondary consequence of hypoxaemia in chronic lung diseases²⁴, we evaluated the effects of PMT on this systemic clinical manifestation. Notably, PMT corrected polycythaemia in *Csf2rb*^{-/-} mice (Fig. 1h).

Finally, we evaluated the effects of PMT on hPAP-associated mortality by comparing the survival of PMT-treated and untreated *Csf2rb*^{-/-} mice. PMT increased the lifespan of *Csf2rb*^{-/-} mice by 107 days, from 555 (median; interquartile range 507–592) days to 662 (604–692) days (Fig. 1i). In separate studies of treated *Csf2rb*^{-/-} mice surviving to 617

(604–631) days (561 (548–575) days after PMT of WT BMDMs), CD131⁺ alveolar macrophages were still present and BAL turbidity remained low compared to untreated *Csf2rb*^{-/-} mice that survived to 631 (631–631) days (optical density at 600 nm (OD_{600}) = 0.75 \pm 0.17 versus 2.63 \pm 0.44; $n = 8, 4$, respectively; $P < 0.001$). However, such long-term evaluation of laboratory abnormalities is obfuscated by reduced survival of untreated *Csf2rb*^{-/-} mice.

These results demonstrate that PMT had a highly efficacious and durable therapeutic effect on the primary pulmonary and secondary systemic manifestations of hPAP in *Csf2rb*^{-/-} mice.

Macrophage engraftment efficiency

We next evaluated the effects of cell dose (0.5, 1, 2 and 4 million) and repeated administration (one versus four monthly transplants) on PMT efficacy (Extended Data Tables 2 and 3, respectively). Neither treatment significantly affected efficacy in the range evaluated, and one dose of 2 million cells was used for PMT in the remaining studies.

To determine whether WT macrophages had a survival advantage over *Csf2rb*^{-/-} macrophages, we measured GM-CSF bioactivity in BAL fluid and found that it was detectable in *Csf2rb*^{-/-} but not WT mice (Extended Data Fig. 1h). WT macrophages had increased survival/proliferation compared to *Csf2rb*^{-/-} macrophages *in vitro* (Fig. 2a) and accumulated to greater numbers after PMT in *Csf2rb*^{-/-} mice than in WT mice (Fig. 2b and Extended Data Fig. 3d). PMT of WT Lys-M^{GFP} knock-in mouse²⁵ BMDMs into *Csf2rb*^{-/-} mice followed by Ki67 immunostaining revealed that PMT-derived cells replicated *in vivo* (Extended Data Fig. 3e–g). The percentage of Ki67⁺ PMT-derived alveolar macrophages was 32.2 \pm 6.05% 1 month after PMT and declined to 11.29 \pm 2.2% by 1 year (Fig. 2c) similar to baseline Ki67⁺ immunostaining of alveolar macrophages in age-matched, normal WT mice (Extended Data Fig. 3f). To define this survival advantage further, we evaluated the engraftment kinetics after one PMT of WT BMDMs in *Csf2rb*^{-/-} mice. CD131⁺ cells increased steadily from zero to 69.0 \pm 2.5% of BAL cells (Fig. 2d) synchronous with a smooth decline in pulmonary GM-CSF to

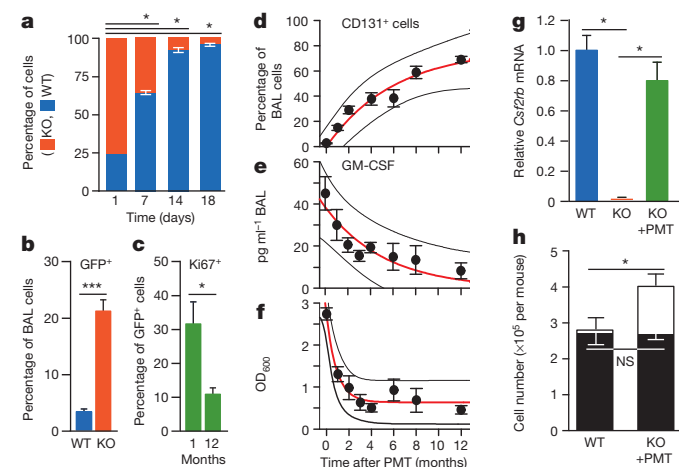


Figure 2 | Pharmacokinetics and pharmacodynamics of PMT in *Csf2rb*^{-/-} mice. **a**, Competitive proliferation of WT and *Csf2rb*^{-/-} BMDMs co-cultured with GM-CSF and M-CSF ($n = 3$ plates per point). **b**, Quantification of GFP⁺ BAL cells 2 months after PMT of Lys-M^{GFP} BMDMs into WT ($n = 3$) or *Csf2rb*^{-/-} ($n = 6$) mice. **c**, Quantification of Ki67⁺ Lys-M^{GFP} cells in *Csf2rb*^{-/-} mice ($n = 3$) 1 or 12 months after PMT. **d–f**, *Csf2rb*^{-/-} mice received PMT of WT BMDMs and were evaluated at the indicated times to quantify CD131⁺ BAL cells (d), BAL GM-CSF concentration (e) and BAL turbidity (f). Exponential regression (\pm prediction bands), $R^2 = 0.943$ (d), $R^2 = 0.819$ (e), $R^2 = 0.958$ (f). Data are mean \pm s.e.m. for 3–7 mice per group. **g**, *Csf2rb* mRNA in BAL cells from *Csf2rb*^{-/-} mice 1 year after PMT, or untreated, age-matched control mice ($n = 6$). **h**, Number of BAL cells (open bars) or CD131⁺ alveolar macrophages (filled bars) in *Csf2rb*^{-/-} mice 1 year after PMT ($n = 5$) or untreated WT mice ($n = 10$). Data are mean \pm s.e.m. * $P < 0.05$, *** $P < 0.001$; NS, not significant.

near normal (Fig. 2e). Similarly, BAL turbidity declined with the increase in CD131⁺ alveolar macrophages (Fig. 2f). One year after PMT, CD131⁺ cells were present (Fig. 1b), CD131 protein (encoded by *Csf2rb*) was detectable in alveolar macrophages (Extended Data Fig. 3a), and *Csf2rb* mRNA in BAL cells from PMT-treated *Csf2rb*^{-/-} mice was only slightly less than in WT and undetectable in untreated *Csf2rb*^{-/-} BAL cells (Fig. 2g). Importantly, numbers of CD131⁺ alveolar macrophages in PMT-treated *Csf2rb*^{-/-} and untreated WT mice were similar 1 year after PMT (Fig. 2h). These results demonstrate that WT macrophages had a selective survival advantage over *Csf2rb*^{-/-} macrophages and that after PMT into *Csf2rb*^{-/-} mice, they proliferated *in vivo* at a rate that slowed over time synchronous with reduction in pulmonary GM-CSF, replaced dysfunctional *Csf2rb*^{-/-} alveolar macrophages, and resulted in numbers of CD131⁺, GM-CSF-responsive alveolar macrophages similar to WT mice.

Macrophage characterization after PMT

The fate of macrophages after PMT was evaluated to determine their spatial distribution, phenotype and gene expression profile. Intra-pulmonary localization was evaluated 1 year after PMT of WT Lys-M^{GFP} BMDMs by fluorescence microscopy to identify CD68⁺GFP⁺ (that is, PMT-derived) macrophages, which revealed that 88.9 ± 0.87% were intra-alveolar and 11.1 ± 0.87% were interstitial (Extended Data Fig. 3h). GFP immunohistochemical staining was done to eliminate potential interference from autofluorescence and confirmed these results; 90.5 ± 1.1% PMT-derived macrophages were intra-alveolar and 9.4 ± 1.1% were interstitial (Fig. 3a, b and Extended Data Fig. 3i). Localization was done in similarly treated mice by flow cytometry to detect GFP⁺ cells 2 months (not shown) or 1 year after PMT (Fig. 3c and Extended Data Fig. 4a, b) and by PCR amplification of Lys-M^{GFP} transgene-specific DNA (Extended Data Fig. 4c), all of which showed that PMT-derived cells were present in the lungs but not detected in blood, bone marrow, or spleen. One year after PMT of CD45.1⁺ WT BMDMs into CD45.2⁺ *Csf2rb*^{-/-} mice, flow cytometric detection of CD45.1⁺ cells confirmed these findings (Extended Data Fig. 4e–g). Results show that the transplanted macrophages remained in the lungs, primarily within the intra-alveolar space.

The effects of the lung environment on the phenotype of transplanted macrophages were evaluated by measuring cell-surface markers. One year after PMT of WT Lys-M^{GFP} BMDMs into *Csf2rb*^{-/-} mice, PMT-derived alveolar macrophages comprised 68.7 ± 6.5% of BAL cells and had converted from CD11b^{Hi}SiglecF^{Low} to CD11b^{Low}SiglecF^{Hi}, similar to the phenotype of WT alveolar macrophages and different from *Csf2rb*^{-/-} mice at the point of PMT (CD11b^{Hi}SiglecF^{Low}) (Fig. 3c, d). Similarly, one year after PMT of WT CD45.1⁺ BMDMs into CD45.2⁺ *Csf2rb*^{-/-} mice, CD45.1⁺ alveolar macrophages comprised 63.6 ± 12.1%

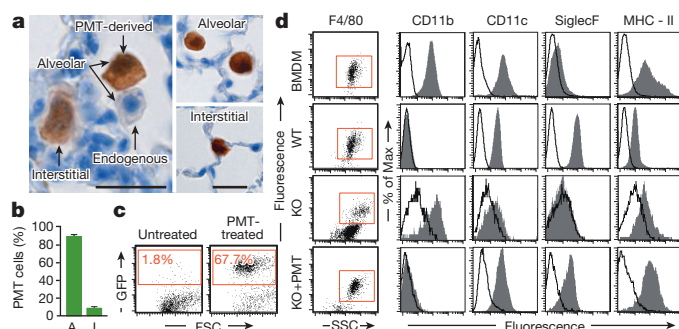


Figure 3 | Localization and phenotype of transplanted macrophages.

Lys-M^{GFP} BMDMs were transplanted into *Csf2rb*^{-/-} mice and evaluated after 1 year. **a**, Immunostained lung showing GFP⁺ cells. Scale bars, left, 200 μm; right, 20 μm. **b**, Localization of GFP⁺ macrophages to intra-alveolar (A) and interstitial (I) spaces ($n = 6$). **c**, GFP⁺ BAL cells identified by flow cytometry. **d**, Phenotypic analysis of F4/80⁺ BMDMs before PMT, and alveolar macrophages from PMT-treated *Csf2rb*^{-/-} mice, or untreated, age-matched WT or *Csf2rb*^{-/-} mice ($n = 6$ per group). Data are mean ± s.e.m.

of BAL cells and had undergone the same phenotypic conversion (Extended Data Fig. 4h).

To determine the effects on gene expression, we performed genome-wide expression profiling on alveolar macrophages from *Csf2rb*^{-/-} mice 1 year after PMT of WT BMDMs and compared to results for untreated, age-matched WT or *Csf2rb*^{-/-} mice. Unsupervised analysis indicated marked co-clustering between PMT-treated *Csf2rb*^{-/-} and WT mice while *Csf2rb*^{-/-} mice clustered separately (Fig. 4). Expression of genes regulated by GM-CSF was reduced in *Csf2rb*^{-/-} mice and restored by PMT (Fig. 4 and Extended Data Fig. 5a). Of 776 genes for which expression was disrupted in *Csf2rb*^{-/-} mice, PMT normalized expression of 600 including 80% of genes upregulated and 76% of genes downregulated in *Csf2rb*^{-/-} compared to WT mice (Extended Data Fig. 5b). Supervised Gene Ontology (GO) and detailed KEGG pathway analysis revealed that genes in multiple pathways involved in lipid metabolism, cellular proliferation, apoptosis and host defence were coordinately downregulated in *Csf2rb*^{-/-} mice, and normalized by PMT (Extended Data Fig. 5c, d). Results for multiple genes important in lipid metabolism (*Abcg1*, *Nrlh3*, *Olr1*, *Lepr*, *Fabp1*, *Lipf*, *Abca1*, *Apoe*, *Apoc2*, *Pla2g7*) were validated using separate samples (Extended Data Fig. 5e).

Efficacy of gene therapy by PMT

Since PMT in humans would probably employ autologous, gene-corrected HSPC-derived macrophages, we evaluated PMT of *Csf2rb*^{-/-} macrophages derived from LSK cells after lentiviral vector (LV)-mediated *Csf2rb* cDNA expression (Fig. 5a). *Csf2rb* gene-corrected (GM-R-LV-transduced) or sham-treated (GFP-LV-transduced) *Csf2rb*^{-/-} and non-transduced WT LSK-derived cells all had macrophage morphology, expressed CD68 (Extended Data Fig. 6a) and were F4/80⁺CD11b^{Hi}CD11c⁺ (not shown). In contrast, only WT and GM-R-LV-transduced *Csf2rb*^{-/-} cells were CD131⁺ and only lentiviral-vector-transduced cells were GFP⁺ (Extended Data Fig. 6a). GM-R-LV restored GM-CSF signalling in *Csf2rb*^{-/-} macrophages (Fig. 5b and Extended Data Fig. 6b). Two months after PMT into *Csf2rb*^{-/-} mice, GM-CSF receptor-β was detected on alveolar macrophages only from mice receiving gene-corrected *Csf2rb*^{-/-} or WT macrophages (Extended Data Fig. 6c). The efficacy using gene-corrected *Csf2rb*^{-/-} or WT cells was equivalent as demonstrated by a similar degree of improvement in BAL appearance (Extended Data Fig. 6d), BAL turbidity, SP-D and biomarkers of hPAP (Fig. 5c, d). Furthermore, gene-corrected BMDMs localized to the lung (Extended Data Fig. 4d and Fig. 6e) and underwent phenotypic conversion to CD11b^{Low} (Extended Data Fig. 6f). The long-term efficacy of gene-corrected macrophages 1 year after PMT was demonstrated by marked reduction in BAL turbidity, SP-D and BAL fluid biomarkers of hPAP (Fig. 5c, d). These results demonstrate that PMT of gene-corrected macrophages had a therapeutic effect on hPAP in *Csf2rb*^{-/-} mice equivalent to that of WT macrophages and was durable, lasting at least 1 year.

Safety of PMT therapy in *Csf2rb*^{-/-} mice

PMT was well tolerated and without adverse effects. One year after PMT, there were no haematological abnormalities (Extended Data Table 4), cellular inflammation or pulmonary fibrosis in mice receiving PMT of WT (Fig. 1d) or gene-corrected macrophages (not shown). *Csf2rb*^{-/-}

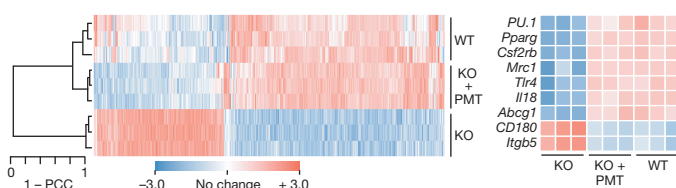


Figure 4 | Microarray analysis of alveolar macrophages 1 year after PMT. Unsupervised hierarchical clustering dendrogram and heat map of selected GM-CSF-regulated genes in PMT-treated *Csf2rb*^{-/-} mice or untreated, age-matched WT or *Csf2rb*^{-/-} mice (3 per group). Pearson correlation coefficient (PCC).

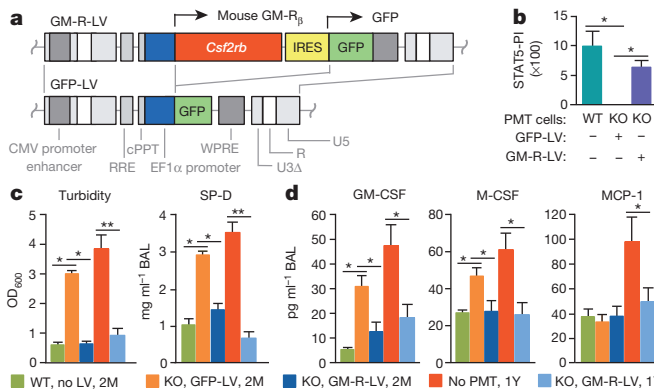


Figure 5 | Effects of PMT of gene-corrected macrophages on hPAP severity and biomarkers. *Csf2rb*^{-/-} mice received PMT of non-transduced WT or lentiviral-vector-transduced *Csf2rb*^{-/-} macrophages and were evaluated after 2 months (2M) or 1 year (1Y) (with untreated, age-matched *Csf2rb*^{-/-} mice). The key indicates PMT cells used, previous lentiviral vector treatment, and time after PMT analysis was performed. **a**, Lentiviral vector schematics. **b**, GM-CSF signalling measured by the STAT5 phosphorylation index (STAT5-PI) in the indicated cells before PMT. **c**, BAL turbidity and SP-D concentration. **d**, BAL biomarkers. Mean \pm s.e.m. of $n = 3$ (**b**) or 5–10 (**c**, **d**) mice per group. * $P < 0.05$, ** $P < 0.01$.

mice had trivial elevations of IL-6 and TNF- α in BAL that were reduced by PMT of WT macrophages (Extended Data Table 4). These data identify no safety concerns for PMT therapy of hPAP in *Csf2rb*^{-/-} mice.

Discussion

Multiple lines of evidence indicate that the high efficacy of PMT therapy of hPAP in *Csf2rb*^{-/-} mice was attributable to a selective survival advantage conferred by increased pulmonary GM-CSF to alveolar macrophages bearing functional GM-CSF receptors. However, pulmonary surfactant remained slightly increased 1 year after a single PMT. This could be because the treatment time was too short or exceeded the durability of the clinical benefit, or due to the continued presence of *Csf2rb*^{-/-} alveolar macrophages despite engraftment of GM-CSF-responsive macrophages. The latter is likely due to ongoing *Csf2rb*^{-/-} myelopoiesis, pulmonary recruitment of monocytes and local proliferation, and GM-CSF-independent survival as occurs in untreated *Csf2rb*^{-/-} mice. *Csf2rb*^{-/-} macrophages may provide a ‘protected intracellular niche’ for surfactant accumulation since without GM-CSF, alveolar macrophages internalize but cannot clear surfactant²⁶. Another factor may be reduction of the survival advantage over time, that is, reduced pulmonary GM-CSF (driving WT cell proliferation) and reduced surfactant burden (driving surfactant-engorgement-related *Csf2rb*^{-/-} cell death). Notwithstanding these points, a single PMT of GM-CSF responsive cells cleared ~90% of the abnormal surfactant accumulation for at least one year.

The feasibility of translating PMT therapy to humans with hPAP is supported by the safety and efficacy of PMT in *Csf2rb*^{-/-} mice and the striking similarity of hPAP in mice and humans. Macrophages could be delivered by bronchoscopic instillation without endotracheal intubation, general anaesthesia, or mechanical ventilation, which are required for whole lung lavage and increase risk. Preparative myeloablation would

be unnecessary and use of autologous, gene-corrected cells would eliminate the need for immunosuppression, which are required for BMT. PMT may also be possible with gene-corrected, inducible pluripotent-cell-derived macrophages recently prepared from children with hPAP^{23,27}. However, formal preclinical toxicology studies related to PMT and to gene transfer will be needed before this approach can be tested in humans. Since pulmonary GM-CSF is critical to lung host defence and clearance of a broad range of microorganisms²⁸, PMT may also be useful in treating serious lung infections. Indeed, pulmonary administration of macrophages constitutively expressing IFN- γ improved host defence in SCID mice²⁹. In such applications, inhaled GM-CSF could be used to promote survival of transplanted macrophages³⁰.

Identification of a homeostatic mechanism by which pulmonary GM-CSF regulates alveolar macrophage population size (Fig. 6) was an unexpected but important finding. Its existence is supported by recent fate-mapping studies indicating that tissue-resident alveolar macrophages derive before birth and self-maintain by local replication independent of circulating monocytes at steady state^{30–33}.

The concept of alveolar macrophages (and other tissue-resident macrophages) as short-lived, terminally differentiated, non-dividing representatives of a unified mononuclear phagocyte system replenished via monocyte intermediates has evolved considerably since its inception³⁴. Alveolar macrophage half-life was initially estimated at 2 weeks based on studies of repopulation after lethal irradiation and allogeneic BMT³⁵. Improved detection methods using GFP⁺ cells increased the estimate to 30 days³⁶. Shielding the thorax during irradiation increased it further to 8 months³⁷. Our data, obtained without irradiation or myeloablation, show that macrophages transplanted directly into the respiratory tract persisted for one-and-a-half years. A caveat of such estimates is their inability to discern if persistence is due to prolonged survival or replication.

Normally, alveolar macrophages are phenotypically CD11b^{Low}SiglecF^{Hi} while other macrophage populations are CD11b^{Hi}SiglecF^{Low}. Surprisingly, WT BMDMs cultured in GM-CSF and M-CSF were CD11b^{Hi}SiglecF^{Low} in vitro but converted to CD11b^{Low}SiglecF^{Hi} after PMT. In contrast, BMDMs instilled in the peritoneum adopt the CD11b^{Hi} phenotype of peritoneal macrophages³⁸. These changes agree with gene-expression profiling studies³⁹ and indicate that local microenvironments provide critical ‘phenotypically instructive’ cues that direct development of tissue-resident macrophage populations. Our results show for alveolar macrophages that GM-CSF provides one such phenotypic cue while the lung environment provides another critical, albeit unidentified, cue.

The limitations of our study include the fact that it did not establish a minimum effective dose, a maximum tolerated dose, or a significant dose-response relationship. BMDMs were capable of clearing surfactant before transplantation but results did not determine whether ‘lung-conditioning’ further increased their clearance capacity. While the macrophages used for PMT contained very few progenitors, it is theoretically possible that clonal expansion of a progenitor subpopulation may have contributed to therapeutic efficacy and, if so, potential clonal shrinkage may have contributed to loss of benefit at later times. Thus, additional studies are needed to further confirm the identity of effector cells and precise pharmacokinetics and durability of the therapeutic benefit.

Online Content Methods, along with any additional Extended Data display items and Source Data, are available in the online version of the paper; references unique to these sections appear only in the online paper.

Received 12 February; accepted 1 September 2014.

Published online 1 October 2014.

1. Suzuki, T. et al. Familial pulmonary alveolar proteinosis caused by mutations in CSF2RA. *J. Exp. Med.* **205**, 2703–2710 (2008).
2. Martinez-Moczygemba, M. et al. Pulmonary alveolar proteinosis caused by deletion of the GM-CSFR α gene in the X chromosome pseudoautosomal region 1. *J. Exp. Med.* **205**, 2711–2716 (2008).
3. Suzuki, T. et al. Hereditary pulmonary alveolar proteinosis: pathogenesis, presentation, diagnosis, and therapy. *Am. J. Respir. Crit. Care Med.* **182**, 1292–1304 (2010).
4. Tanaka, T. et al. Adult-onset hereditary pulmonary alveolar proteinosis caused by a single-base deletion in CSF2RB. *J. Med. Genet.* **48**, 205–209 (2011).

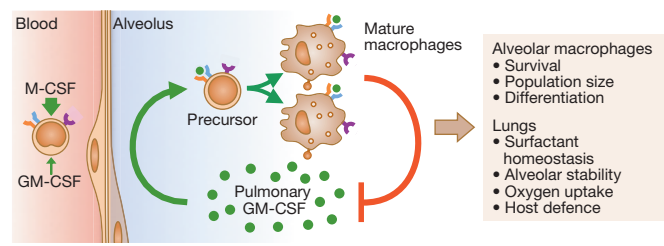


Figure 6 | Proposed homeostatic reciprocal feedback mechanism by which pulmonary GM-CSF regulates alveolar macrophage population size in vivo.

5. Suzuki, T. et al. Hereditary pulmonary alveolar proteinosis caused by recessive CSF2RB mutations. *Eur. Respir. J.* **37**, 201–204 (2011).
6. Whitsett, J. A., Wert, S. E. & Weaver, T. E. Alveolar surfactant homeostasis and the pathogenesis of pulmonary disease. *Annu. Rev. Med.* **61**, 105–119 (2010).
7. Hawgood, S. & Poulain, F. R. The pulmonary collectins and surfactant metabolism. *Annu. Rev. Physiol.* **63**, 495–519 (2001).
8. Ikegami, M. et al. Surfactant metabolism in transgenic mice after granulocyte macrophage-colony stimulating factor ablation. *Am. J. Physiol.* **270**, L650–L658 (1996).
9. Kitamura, T. et al. Idiopathic pulmonary alveolar proteinosis as an autoimmune disease with neutralizing antibody against granulocyte/macrophage colony-stimulating factor. *J. Exp. Med.* **190**, 875–880 (1999).
10. Trapnell, B. C., Whitsett, J. A. & Nakata, K. Pulmonary alveolar proteinosis. *N. Engl. J. Med.* **349**, 2527–2539 (2003).
11. Stanley, E. et al. Granulocyte/macrophage colony-stimulating factor-deficient mice show no major perturbation of hematopoiesis but develop a characteristic pulmonary pathology. *Proc. Natl Acad. Sci. USA* **91**, 5592–5596 (1994).
12. Dranoff, G. et al. Involvement of granulocyte-macrophage colony-stimulating factor in pulmonary homeostasis. *Science* **264**, 713–716 (1994).
13. Robb, L. et al. Hematopoietic and lung abnormalities in mice with a null mutation of the common beta subunit of the receptors for granulocyte-macrophage colony-stimulating factor and interleukins 3 and 5. *Proc. Natl Acad. Sci. USA* **92**, 9565–9569 (1995).
14. Nishinakamura, R. et al. Mice deficient for the IL-3/GM-CSF/IL-5 βc receptor exhibit lung pathology and impaired immune response, while βIL3 receptor-deficient mice are normal. *Immunity* **2**, 211–222 (1995).
15. Bonfield, T. L. et al. Peroxisome proliferator-activated receptor-γ is deficient in alveolar macrophages from patients with alveolar proteinosis. *Am. J. Respir. Cell Mol. Biol.* **29**, 677–682 (2003).
16. Bonfield, T. L. et al. PU.1 regulation of human alveolar macrophage differentiation requires granulocyte-macrophage colony-stimulating factor. *Am. J. Physiol. Lung Cell. Mol. Physiol.* **285**, L1132–L1136 (2003).
17. Seymour, J. F. & Presneill, J. J. Pulmonary alveolar proteinosis: progress in the first 44 years. *Am. J. Respir. Crit. Care Med.* **166**, 215–235 (2002).
18. Shibata, Y. et al. GM-CSF regulates alveolar macrophage differentiation and innate immunity in the lung through PU.1. *Immunity* **15**, 557–567 (2001).
19. Thomassen, M. J. et al. ABCG1 is deficient in alveolar macrophages of GM-CSF knockout mice and patients with pulmonary alveolar proteinosis. *J. Lipid Res.* **48**, 2762–2768 (2007).
20. Iyonaga, K. et al. Elevated bronchoalveolar concentrations of MCP-1 in patients with pulmonary alveolar proteinosis. *Eur. Respir. J.* **14**, 383–389 (1999).
21. Nishinakamura, R. et al. The pulmonary alveolar proteinosis in granulocyte-macrophage colony-stimulating factor/interleukins 3/5 beta c receptor-deficient mice is reversed by bone marrow transplantation. *J. Exp. Med.* **183**, 2657–2662 (1996).
22. Kleff, V. et al. Gene therapy of βc-deficient pulmonary alveolar proteinosis (βc-PAP): studies in a murine *in vivo* model. *Mol. Ther.* **16**, 757–764 (2008).
23. Suzuki, T. et al. Use of induced pluripotent stem cells to recapitulate pulmonary alveolar proteinosis pathogenesis. *Am. J. Respir. Crit. Care Med.* **189**, 183–193 (2014).
24. Stradling, J. R. & Lane, D. J. Development of secondary polycythaemia in chronic airways obstruction. *Thorax* **36**, 321–325 (1981).
25. Faust, N., Varas, F., Kelly, L. M., Heck, S. & Graf, T. Insertion of enhanced green fluorescent protein into the lysozyme gene creates mice with green fluorescent granulocytes and macrophages. *Blood* **96**, 719–726 (2000).
26. Yoshida, M., Ikegami, M., Reed, J. A., Chroneos, Z. C. & Whitsett, J. A. GM-CSF regulates surfactant Protein-A and lipid catabolism by alveolar macrophages. *Am. J. Physiol. Lung Cell. Mol. Physiol.* **280**, L379–L386 (2001).
27. Lachmann, N. et al. Gene correction of human induced pluripotent stem cells repairs the cellular phenotype in pulmonary alveolar proteinosis. *Am. J. Respir. Crit. Care Med.* **189**, 167–182 (2014).
28. Seymour, J. F. et al. Mice lacking both granulocyte colony-stimulating factor (CSF) and granulocyte-macrophage CSF have impaired reproductive capacity, perturbed neonatal granulopoiesis, lung disease, amyloidosis, and reduced long-term survival. *Blood* **90**, 3037–3049 (1997).
29. Wu, M. et al. Genetically engineered macrophages expressing IFN-γ restore alveolar immune function in scid mice. *Proc. Natl Acad. Sci. USA* **98**, 14589–14594 (2001).
30. Guilliams, M. et al. Alveolar macrophages develop from fetal monocytes that differentiate into long-lived cells in the first week of life via GM-CSF. *J. Exp. Med.* **210**, 1977–1992 (2013).
31. Hashimoto, D. et al. Tissue-resident macrophages self-maintain locally throughout adult life with minimal contribution from circulating monocytes. *Immunity* **38**, 792–804 (2013).
32. Yona, S. et al. Fate mapping reveals origins and dynamics of monocytes and tissue macrophages under homeostasis. *Immunity* **38**, 79–91 (2013).
33. Schulz, C. et al. A lineage of myeloid cells independent of Myb and hematopoietic stem cells. *Science* **336**, 86–90 (2012).
34. van Furth, R. & Cohn, Z. A. The origin and kinetics of mononuclear phagocytes. *J. Exp. Med.* **128**, 415–435 (1968).
35. Godleski, J. J. & Brain, J. D. The origin of alveolar macrophages in mouse radiation chimeras. *J. Exp. Med.* **136**, 630–643 (1972).
36. Matute-Bello, G. et al. Optimal timing to repopulation of resident alveolar macrophages with donor cells following total body irradiation and bone marrow transplantation in mice. *J. Immunol. Methods* **292**, 25–34 (2004).
37. Murphy, J., Summer, R., Wilson, A. A., Kotton, D. N. & Fine, A. The prolonged life-span of alveolar macrophages. *Am. J. Respir. Cell Mol. Biol.* **38**, 380–385 (2008).
38. Guth, A. M. et al. Lung environment determines unique phenotype of alveolar macrophages. *Am. J. Physiol. Lung Cell. Mol. Physiol.* **296**, L936–L946 (2009).
39. Gautier, E. L. et al. Gene-expression profiles and transcriptional regulatory pathways that underlie the identity and diversity of mouse tissue macrophages. *Nature Immunol.* **13**, 1118–1128 (2012).

Acknowledgements This work was supported by grants from the NIH (R01 HL085453, R21 HL106134, R01 HL118342, 8UL1TR000077-05, AR-47363, DK78392, DK90971), American Thoracic Society Foundation Unrestricted Research Grant, CCHMC Foundation Trustee Grant, Deutsche Forschungsgemeinschaft (DFG; Cluster of Excellence Rebirth; Exz 62/1), the Else Kröner Fresenius Stiftung, the Eva-Luise Koehler Research Prize for Rare Diseases 2013, and by the Pulmonary Biology Division, CCHMC. Flow cytometric data were acquired within the Research Flow Cytometry Core in the Division of Rheumatology, CCHMC. We thank our hPAP patients and their family members in the United States and internationally for their collaboration; J. Whitsett (CCHMC) and F. McCormack (UCMC) for critical reading of the manuscript; J. Krischer (University of South Florida) and Y. Maeda (CCHMC) for helpful discussions; S. Wert for help with lung histology; and D. Black, K. Link and C. Fox (CCHMC), and S. Brennig and H. Kempf (Hannover Medical School) for their technical help.

Author Contributions T.Su., P.A., N.L., S.A., T.M., P.M. and B.C.T. designed research. T.Su., P.A., T.Sa., N.L., C.C., A.S., S.A., B.C. and B.C.T. performed research. T.Su., P.A., T.Sa., N.L., S.A., C.T., T.M., P.M. and B.C.T. analysed data. T.Su., P.A., N.L., P.M., C.L., R.E.W. and B.C.T. wrote the paper.

Author Information Reprints and permissions information is available at www.nature.com/reprints. Microarray data are available at Gene Expression Omnibus under accession number GSE60528. The authors declare no competing financial interests. Readers are welcome to comment on the online version of the paper. Correspondence and requests for materials should be addressed to B.T. (Bruce.Trapnell@cchmc.org) or T.Su. (Takuji.Suzuki@cchmc.org).

METHODS

Mice. All mice were bred, housed and studied in the Cincinnati Children's Research Foundation Vivarium using protocols approved by the Institutional Animal Care and Use Committee. *Csf2rb* gene-targeted (*Csf2rb*^{-/-}) mice¹³, and mice expressing EGFP knocked into the lysozyme M gene (Lys-M^{GFP} mice)²⁵, were all generated previously and backcrossed onto the C57BL/6 background. C57BL/6 mice (referred to as wild type or WT mice) were purchased from Charles River. B6.SJL-*Ptprc*^a*Pepc*^b/BoyJ (CD45.1⁺) mice were from Jackson Laboratory.

Lung histology and immunohistochemistry. Animals were killed by intraperitoneal pentobarbital administration and exsanguination by aortic transection. The trachea was exposed by a vertical midline skin incision, cannulated through a small transverse incision in its ventral surface away from the thoracic inlet, inflated with fixative (PBS, pH 7.4, containing 4% paraformaldehyde) under a hydrostatic head of 25 cm and ligated with suture while retracting the cannula to seal the lung under pressure. The sternum and diaphragm were transected sagittally, retracted laterally, and the lungs and heart separated from the chest wall by blunt dissection to avoid puncturing the mediastinal pleura and removed from the chest. The intact tissue block containing the heart, lungs and ligated trachea was submerged in fixative and kept at 4 °C for 24 h. After fixation, the lung lobes were divided, removed from the tissue block, cut into ~2-mm-thick slices along the long axis, washed in cold PBS, dehydrated, embedded in paraffin, and 5-μm-thick sections were cut and stained with haematoxylin and eosin (H&E), periodic acid-Schiff reagent (PAS), or Masson's trichrome as previously described⁴⁰. Immunostaining for surfactant protein B (SP-B) was done by incubating slides with rabbit anti-SP-B polyclonal antibody (diluted 1:500, Seven Hills Bioreagents, Cincinnati, OH) and Vectastain ABC anti-rabbit immunohistochemical horseradish peroxidase kit (Vector Labs, Inc., Burlingame, CA) and counterstaining with haematoxylin as described⁴¹. To prepare frozen lung sections, the lungs were inflation fixed *in situ* as described above and then the heart and lungs were removed en bloc and cryoprotected by sequential immersion in PBS containing increasing sucrose concentrations (10%, 15% and 20%; 8–12 h, 4 °C, at each concentration). The lungs were then embedded in Tissue-Tek OCT compound (Sakura Finetek, Torrance, CA), frozen and stored at –80 °C until use. Serial 6 μm sections were prepared for immunostaining or evaluation of GFP⁺ cells. Lung sections and sedimented lung cells were examined by light microscopy using a Zeiss Axioplan 2 microscope (Zeiss) equipped with AxioVision software (Zeiss).

Collection, handling and evaluation of bronchoalveolar lavage fluid and cells. Epithelial lining fluid and non-adherent cells were collected from lung surface of mice by bronchoalveolar lavage (BAL) as described⁴² and processed immediately. Briefly, five 1-ml aliquots were instilled and immediately recovered per mouse and combined resulting in a BAL recovery of 93.9 ± 1.2% per mouse (BAL recovery data for 10 mice evaluated randomly). The photographs of fresh BAL specimens and the specimen after allowing sediment to be formed by overnight incubation at 4 °C were taken. The turbidity of BAL was determined as described⁴¹. Briefly, after gently mixing to ensure a homogeneous suspension of BAL, a 250 μl aliquot was diluted into 750 μl PBS and the optical density was measured at a wavelength of 600 nm and multiplying the result by the dilution factor. The total number of BAL cells recovered from each mouse was determined by counting cells in an aliquot of known volume using a haemocytometer and multiplying the result by the total volume of BAL and dividing by the volume of the aliquot used for counting. BAL cytology was evaluated in aliquots (~50,000 cells) after sedimentation (Cytopsin, Shandon, Inc.; 500 r.p.m., 7 min, room temperature) onto glass slides and staining with DiffQuick, PAS, or oil red O (all from Fisher Scientific) as described⁴¹. The cell differential was determined by microscopic examination of DiffQuick stained cells and the total number of alveolar macrophages per mouse was determined by multiplying the percentage of alveolar macrophages in BAL cells by the total number of BAL cells recovered⁴³. BAL fluid and cells were separated by low-speed centrifugation (285g, 10 min, room temperature) and stored at –80 °C until use (BAL fluid) or immediately evaluated (referred to as BAL cells) or used to isolate alveolar macrophages (see below). Primary alveolar macrophages were purified by brief adherence of BAL cells to plastic as described¹⁸. Viability was evaluated by Trypan blue exclusion and was ≥95%.

ELISA. The concentration of surfactant protein D (SP-D) in BAL fluid was measured by enzyme-linked immunosorbent assay (ELISA) as we described⁴¹. The concentration of several cytokines (GM-CSF, M-CSF, MCP-1, IL-1β, IL-6, TNF-α) in BAL fluid and erythropoietin in serum was measured by ELISA (Mouse Quantikine Kits, R&D Systems) as described¹.

Quantitative RT-PCR. Total RNA was isolated from alveolar macrophages using TRIzol Reagent (Life Technologies, Carlsbad, CA) and then used to purify mRNA using RNeasy (Qiagen, Valencia, CA), both as directed by the manufacturers. Purified mRNA was used to synthesize cDNA using the Invitrogen SuperScript III First-Strand Synthesis System (Life Technologies). Standard quantitative RT-PCR (qRT-PCR) was performed as previously described¹ on an Applied Biosystems 7300 Real-Time PCR System (Life Technologies) to measure transcript abundance using

TaqMan oligonucleotide primer sets (all from Life Technologies) (Extended Data Table 1). Expression of target genes was normalized to the expression of 18s RNA. Data for each gene were shown as the fold change of the mean of results for wild-type mice.

Bone-marrow-derived macrophages (BMDMs). Bone marrow cells were obtained from 6–8-week-old WT, *Csf2rb*^{-/-}, or Lys-M^{GFP} mice by isolating and flushing tibias and femurs with DMEM (Life Technologies) containing 10% heat-inactivated FBS, 50 U ml⁻¹ penicillin, and 50 μg ml⁻¹ streptomycin. After red blood cells were removed with BD Pharm Lyse (BD Biosciences), mononuclear cells were isolated by centrifugation on Ficoll-Paque (GE Healthcare) at room temperature for 30 min, washed, re-suspended in DMEM containing 10% heat-inactivated FBS, 50 U ml⁻¹ penicillin, 50 μg ml⁻¹ streptomycin, 10 ng ml⁻¹ GM-CSF and 5 ng ml⁻¹ M-CSF (both from R&D Systems), seeded into plastic dishes (Falcon) at a density of ~27 × 10⁶ cells per 10 cm dish (1 per mouse) and cultured overnight at 37 °C in a humidified environment containing 5% CO₂. The next day, non- or weakly-adherent cells were recovered, transferred to a new dish and cultured under the conditions just described to permit differentiation and expansion of macrophages; firmly adherent cells were discarded. After 2 days the culture medium was changed and after 5 days from seeding, adherent bone-marrow-derived macrophages were gently washed with PBS, harvested by brief exposure to trypsin-EDTA (Life Technologies), washed, and used for experiments. The cell purity was high as indicated by the percentage of CD68⁺ and F4/80⁺ cells (96.6 ± 0.3%, 95.4 ± 1.3%, respectively, not shown).

Some experiments used lineage-negative (Lin⁻) c-Kit⁺Sca-1⁺ (LSK) cells which were obtained from mouse bone marrow as described⁴⁴. Briefly, bone marrow from 6–8-week-old WT or *Csf2rb*^{-/-} mice was collected as above and lineage depleted with biotinylated lineage antibodies CD5 (53-7.3), CD8a (53-6.7), CD45R/B220 (RA3-6B2), CD11b (M1/70), Gr-1 (RB6-8C5), and TER-119 (TER-119) (BD Bioscience), and magnetic beads (Dynabeads sheep anti-rat IgG) (Life Technologies). After removing lineage-positive cells, the remaining cells were stained with 7-ADD, FITC-Streptavidin (BD Biosciences) and antibodies to Sca-1 (D7) and c-Kit (2B8) (BD Biosciences). Then, Lin⁻c-Kit⁺Sca-1⁺7-ADD⁻ cells were isolated by cell sorting on a FACSAria (BD Biosciences) and used immediately in experiments. Cell morphology was confirmed by DiffQuick Staining of sedimented cells (Cytopsin, Shandon) and viability was measured by Trypan blue exclusion as described¹⁸ and found to be ≥95%. In some experiments, cells were immunostained for CD68 (FA-11) (AbD Serotec), counterstained with DAPI as described⁴¹, and examined by light microscopy using a Zeiss Axioplan 2 microscope (Zeiss) equipped with AxioVision software (Zeiss).

Colony forming cell (CFC) assay. BMDMs or Lin⁻ bone marrow cells were evaluated for the presence of hematopoietic progenitors capable of forming colonies in semisolid medium in response to cytokine stimulation as previously described⁴⁵. Briefly, fresh Lin⁻ bone marrow cells or BMDMs after induced differentiation into macrophages for 5 days were seeded into standard mouse methylcellulose media supplemented with insulin, transferrin, SCF, IL-3, IL-6 and erythropoietin (HSC007, R&D Systems, Minneapolis, MN). After 7 days in culture, colonies of ≥50 cells were visible and were examined morphologically using whole-plate stack images acquired using an AXIO-Z1 microscope and AXIO-vision software (Zeiss, Jena, Germany) to identify and enumerate burst-forming erythroid progenitors (BFU-E), colony-forming myeloid progenitors (CFU-GM) and the multi-potential progenitors (CFU-GEMM).

Surfactant clearance assay. BMDMs were evaluated functionally to demonstrate their ability to clear human surfactant as we previously reported⁴¹. Briefly, BMDMs from either WT or *Csf2rb*^{-/-} mice were seeded into 12-well plates (4 × 10⁵ cells per well) in DMEM, 10% FBS, 10 ng ml⁻¹ GM-CSF, 5 ng ml⁻¹ M-CSF. Human surfactant recovered by lavage of a patient with PAP was added to the media and cells were incubated for 24 h to permit surfactant uptake into cells and then washed to remove extracellular surfactant. Cells were incubated for 24 h to permit macrophages to clear internalized surfactant. Cells collected before, immediately after surfactant exposure or 24 h after the completion of surfactant exposure were sedimented onto slides by cytocentrifugation (Shandon), stained with oil red O, and counterstained with haematoxylin. Oil red O staining was evaluated in ≥10 random 20× microscopic fields for each sample as described⁴¹.

Pulmonary macrophage transplantation (PMT). BMDMs or LSK cell-derived macrophages were administered directly into the lungs of 8-week-old mice using a relatively non-invasive endotracheal instillation method described previously⁴⁶. Briefly, mice received light anaesthesia by isoflurane inhalation and were suspended on a flat board by a rubber band across the upper incisors and placed in a semi-recumbent (45°) position with the ventral surface and rostrum facing upwards. Using a curved blade Kelly forceps, the tongue was gently and partially retracted rostrally, and 50 μl of PBS containing the macrophages to be administered was placed in the back of the oral cavity using a micropipette. The PBS and cells were inhaled into the lungs by subsequent respiratory efforts under direct visualization. Mice were then observed while recovering from anaesthesia to ensure continued

retention of the administered fluid and cells and then returned to their cages for routine care and handling. Because the efficacy of PMT at a dose of two million macrophages was optimal, this dose given as one administration was used throughout the study except where noted (Extended Data Tables 2 and 3). Age-matched mice were used in all experiments to control for the degree of lung disease severity.

Flow cytometry. BAL cells were purified by centrifugation on Percoll to remove surfactant and debris³¹. BAL cells or BMDMs were immunostained to detect CD115 (AFS98), F4/80 (BM8) (eBioscience), CD3 (145-2C11), CD11b (M1/70), CD11c (HL3), CD16/32 (2.4G2), CD19 (1D3), CD64 (X54-5/7.1.1), CD131 (JORO50), Ly6G (1A8), CD45.1 (A20), CD45.2 (104), MHC class II (I-A/I-E) (M5/114.15.2), SiglecF (E50-2440) (BD Biosciences), CD14 (Sa14-2) (BioLegend), CD68 (FA-11) (AbD Serotec), and MerTK (108928) (R&D Systems), as previously described¹, evaluated by flow cytometry using a FACSCaliber or FACSCanto flow cytometers (both from BD Biosciences, San Jose, CA), and the results were analysed using CellQuest, FACSDiva (BD Biosciences), or FlowJo software (Tree Star). For intracellular staining of CD68, Leucoperm (AbD Serotec) was used as directed by the manufacturer.

Quantification of CD131⁺ alveolar macrophages. The percentage of BAL cells expressing the GM-CSF receptor β-subunit was determined by immunostaining. Briefly, aliquots of BAL cells were sedimented onto glass slides and incubated (10 min, room temperature) in fixative (PBS containing 4% paraformaldehyde), washed with PBS and incubated (4 °C, overnight) with anti-mouse GM-CSF receptor-β (CD131) antibody (sc-678) (Santa Cruz) diluted 1:400 in PBST (PBS containing 2.5% (w/v) Triton X-100 and 5% (v/v) goat serum). After incubation, slides were rinsed five times in PBST and incubated (room temperature, 1 h) with the secondary detection antibody (Alexa-Fluor-594-conjugated, anti-rabbit IgG (Life Technologies)) and counterstained with 4',6-diamidino-2-phenylindole dihydrochloride (DAPI) (Vector Labs, Burlingame, CA). Cells were examined using a Zeiss Axioplan 2 microscope (Zeiss) equipped with AxioVision software (Zeiss). The percentage of CD131⁺ BAL cells was determined by first counting the CD131⁺ and DAPI⁺ cells in five (or more) random 20× microscopic fields for each BAL sample. Then, the number of CD131⁺ cells in each field was divided by the number of DAPI⁺ cells in the same field and results for all fields examined were averaged and multiplied by 100. The total number of CD131⁺ cells per mouse was calculated by multiplying the percentage of CD131⁺ cells by the total number of BAL cells recovered from each mouse.

STAT5 phosphorylation index assay. GM-CSF bioactivity in BAL fluid and GM-CSF receptor function in transduced or WT macrophages was evaluated by measuring GM-CSF-stimulated phosphorylation of STAT5 in BMDMs or LSK cell-derived macrophages using anti-phospho STAT5 antibody (47/Stat5(pY694)) (BD Biosciences) by flow cytometry as previously reported¹. The STAT5 phosphorylation index (STAT5-PI) was calculated as the mean fluorescence intensity of phosphorylated STAT5 staining in GM-CSF-stimulated cells minus that of non-stimulated cells, divided by that of non-stimulated cells, and multiplied by 100. In experiments to quantify GM-CSF bioactivity, WT BMDMs were incubated in BAL fluid containing anti-GM-CSF (22E9, eBioscience) or isotype control antibody (10 µg ml⁻¹) for 30 min and then evaluated.

Evaluation of macrophage proliferation. *In vitro mixed-cell proliferation assay.* CD45.1⁺ WT LSK-derived cells and CD45.2⁺ Csf2rb^{-/-} LSK-derived cells were isolated, seeded into dishes at an initial ratio of 1:3, respectively, and cultured in DMEM containing 10% bovine calf serum, 1% penicillin/streptomycin, GM-CSF (10 ng ml⁻¹) and M-CSF (5 ng ml⁻¹). Cells were collected at 1, 7, 14 and 18 days, immunostained with anti-murine CD45.1, anti-CD45.2 and evaluated by flow cytometry to determine the percentage of each cell type at these times.

In vivo evaluation of transplanted macrophage proliferation. Frozen lung tissue sections were immunostained with anti-Ki67 antibody (Roche) and examined using a Zeiss Axioplan 2 microscope (Zeiss). The percentage of proliferating PMT-derived cells was determined by enumerating GFP⁺ Ki67⁺ cells among total GFP⁺ cells in ≥ 7 random 20× microscopic fields for each sample. To confirm the specificity of Ki67 immunostaining, paraffin-embedded sections or WT alveolar macrophages isolated by BAL and adherence were also stained with Ki67 and examined by light microscopy.

Western blotting. Detection of GM-CSF receptor-β and actin by western blotting was done as previously described¹ with the following modifications. Briefly, primary alveolar macrophages (0.5×10^6 per condition) or cultured BMDMs (1×10^6 per condition) were collected by low-speed centrifugation (285g, 4 °C, 10 min) and the pellets incubated on ice for 30 min in 200 µl of lysis buffer (50 mM Tris-HCl pH 8.0, 150 mM NaCl, 1% (v/v) nonidet p-40, 0.5% (w/v) sodium deoxycholate, 0.1% (w/v) sodium dodecyl sulphate (SDS), 0.004% (w/v) sodium azide) containing 2% (v/v) proteinase inhibitor cocktail (phenyl-methyl-sulphonyl-fluoride and sodium orthovanadate; Santa Cruz). Insoluble debris was removed by centrifugation at 10,000g, 4 °C, 15 min and the supernatant transferred to a clean polypropylene tube. An equal volume of Laemmli sample loading buffer (Bio-Rad, CA) was added and the tubes were capped tightly, vortexed briefly, boiled for 5 min, and separated by electrophoresis on SDS-polyacrylamide gradient (4–12%) gels

(Invitrogen) under reducing conditions. Separated proteins were transferred to PVDF membranes by electro-blotting, incubated in blotting solution (50 mM Tris-HCl pH 8.0, 150 mM NaCl, 5% (w/v) non-fat dry milk (Kroger, Cincinnati, OH), 0.1% (v/v) Tween 20; 4 °C, overnight) to block non-specific binding. Diluted primary detection antibody (see below) was added and the membranes were incubated for 2 h at room temperature and then washed in TBST (50 mM Tris-HCl pH 8.0, 150 mM NaCl, 0.1% (v/v) Tween 20). Membranes were then incubated with the secondary HRP-conjugated detection antibody in blotting solution for 1 h at room temperature and then washed as above and then incubated with ECL-Plus (GE Healthcare) as directed by the manufacturer. Anti-mouse GM-CSF receptor-β antibody (sc-678) (Santa Cruz) diluted 1:500 and anti-actin (sc-1616) (Santa Cruz) diluted 1:1,000 were used for primary antibodies.

Haematological analysis. Blood was obtained from the superior vena cava from mice and 20 µl was used to measure complete blood counts on a fully automated Hemavet 850 (Drew Scientific). Data for the precision and linearity of measurements made with the Hemavet850 can be found online at http://www.drewscientific.com/product_hemavet850.htm.

Microarray analysis. Alveolar macrophages were obtained from age-matched mice (three per condition) and analysed individually as follows. Total RNA was isolated as described above and microarray analysis was performed using the Mouse Gene 1.0 ST Array (Affymetrix, Santa Clara, CA) in the CCHMC Affymetrix Core using standard procedures as described⁴⁷. Data (available at Gene Expression Omnibus accession GSE60528) were analysed using the Affymetrix package in the R statistical programming language (Bioconductor; <http://www.bioconductor.org>). Probes were corrected for background using the Microarray Analysis Suite algorithm, quantile normalized, and probe sets were summarized using the average difference of perfect matches only. Differential expression tests were performed using significance analysis of microarrays⁴⁸ with Benjamini-Hochberg correction for multiple testing⁴⁹. Significant gene lists were selected with a Δ that constrained the false discovery rate to less than 10%. Cluster dendrogram was generated from unsupervised hierarchical clustering analysis of microarray data from probes for all 28,853 genes represented on the chip (Spearman correlation; 3 mice per group). In Venn diagrams, numbers of genes for which expression was altered in alveolar macrophages from Csf2rb^{-/-} compared to WT mice (WT → KO) or PMT-treated compared to untreated Csf2rb^{-/-} mice (KO → KO + PMT) were shown. Only genes with statistically significant changes (false detection rate <10%) of at least twofold were marked as increased (up arrows) or decreased (down arrows). The numbers of genes for which expression was disrupted in Csf2rb^{-/-} mice and normalized by PMT (or unchanged in both comparisons) is shown in the overlap regions. In gene ontology analysis, data show the coordinate increases (red) or decreases (blue) in expression of genes in all gene sets significant at or below a false detection rate of 10% calculated by the Gene Set Test with correction for multiple testing.

Lentiviral vectors, LSK-cell transduction, and differentiation and expansion of transduced macrophages. Gene transfer vectors were constructed using routine methods⁴⁴ from the vector backbone of (Ery-GFP), a human immunodeficiency virus-based, self-inactivating (SIN) lentiviral vector (LV) harbouring a 398-bp U3 deletion eliminating the strong viral promoter/enhancer element⁵⁰. GM-R-LV contains a chimaeric transgene comprised of the human elongation factor 1-α (ELF1-α) promoter (a 1,189-bp fragment containing intron 1 ending 20 bp upstream of the ATG codon isolated from the pEF-BOS plasmid⁵¹) followed by the mouse Csf2rb cDNA (nucleotides –80 to 2,691, GenBank accession number M34397.1) located 3' of the lentiviral central poly-purine tract and followed by an internal ribosome binding site (IRES) and then an enhanced green fluorescent protein (GFP) transgene (Fig. 5a). GFP-LV is a lentiviral vector of similar design except that the Csf2rb and IRES were omitted and the GFP transgene is driven from the ELF1-α promoter (Fig. 5a). Both vectors contain a viral splice donor site, packaging sequence, splice acceptor site, and central polypyrimidine tract (cPPT) 5' of the ELF1-α promoter and a woodchuck hepatitis post-transcriptional regulatory element (WPRE) (nucleotides 1093 to 1684; GenBank accession number J04514)⁵² located 3' of the GFP stop codon as described⁵⁰. Lentiviral vectors were produced by transient transfection as vesicular stomatitis virus-G (VSVG) virions, concentrated, and titred as described⁴⁴. Csf2rb^{-/-} LSK cells were isolated, transduced and expanded as described⁵³ except that transductions were done at a multiplicity of infection (MOI) of 20 for two 12-h periods, IL-11 was omitted, GM-CSF (10 ng ml⁻¹) and M-CSF (5 ng ml⁻¹) were included, SCF and Flt-3 ligand were sequentially reduced (50, 1, 0 ng ml⁻¹), and IL-3 was present early.

Transduction, expansion and differentiation of LSK cells into gene-corrected macrophages was done by adjusting the cytokine ‘cocktail’ mixture to optimize the culture conditions for each of four sequential stages, which included: (1) LSK transduction: murine SCF (R&D) 50 ng ml⁻¹, mIL-3 (PeproTech) 10 ng ml⁻¹, hFlt3-L (PeproTech) 50 ng ml⁻¹ and GM-CSF (R&D) 10 ng ml⁻¹, culture time of two 12-h periods; (2) progenitor expansion: mSCF 50 ng ml⁻¹, hFlt3-L 50 ng ml⁻¹ and GM-CSF 10 ng ml⁻¹, culture time of 4 days; (3) macrophage lineage commitment: mSCF 1 ng ml⁻¹, hFlt3-L 1 ng ml⁻¹, GM-CSF 10 ng ml⁻¹, M-CSF (R&D) 5 ng ml⁻¹, culture

time of 3 days; and (4) macrophage differentiation: GM-CSF 10 ng ml⁻¹ and M-CSF 5 ng ml⁻¹, culture time of 4 days. StemSpan (STEMCELL Technologies) containing 2% FBS, 1% penicillin/streptomycin, 10 mM dNTP, and low-density lipoprotein was used as the culture medium for the LSK transduction and DMEM with 10% FBS, 50 U ml⁻¹ penicillin and 50 µg ml⁻¹ streptomycin was used for all other stages. Phenotype markers (F4/80, CD11b, CD11c) were analysed by flow cytometry at each stage to monitor macrophage differentiation. Only adherent macrophages at the end of this procedure were used for PMT.

Localization of PMT-derived cells after transplantation. Several approaches were used to identify and localize PMT-derived cells within the lung parenchyma and in different organs.

Intra-pulmonary localization of PMT-derived cells. CD131 immunostaining and fluorescence microscopy or flow cytometry was used to detect and quantify transplantation-derived donor macrophages among BAL cells from the lungs of *Csf2rb*^{-/-} mice that previously received PMT of WT (C57BL/6) BMDMs, Lys-M^{GFP} BMDMs, CD45.1⁺ WT BMDMs, or GM-R-GFP-LV *Csf2rb* gene-corrected *Csf2rb*^{-/-} LSK-derived macrophages.

To localize PMT-derived macrophages to intra-alveolar space or interstitium of the lung, frozen lung sections from mice that received PMT of Lys-M^{GFP} BMDMs 1 month or 1 year earlier were immunostained with CD68, counterstained with DAPI (Vector Labs) and evaluated by fluorescence microscopy to identify macrophages, PMT-derived cells, and nucleated cells, respectively. PMT-derived macrophages (that is, GFP⁺CD68⁺ cells) located within the intra-alveolar space or the interstitium were then enumerated. To eliminate the possibility of any interference from non-specific auto-fluorescence of alveolar macrophages, paraffin-embedded lung sections from these mice were immunostained with anti-GFP antibody (Life Technologies) and examined by light microscopy to enumerate immunohistochemically marked macrophages located within the intra-alveolar space or interstitium.

Organ-specific localization of PMT-derived cells. In one approach, *Csf2rb*^{-/-} mice received PMT of Lys-M^{GFP} BMDMs and 1 year later, cells isolated from the BAL, blood, bone marrow, and spleen were evaluated by flow cytometry to detect GFP⁺ cells as a marker for PMT-derived cells.

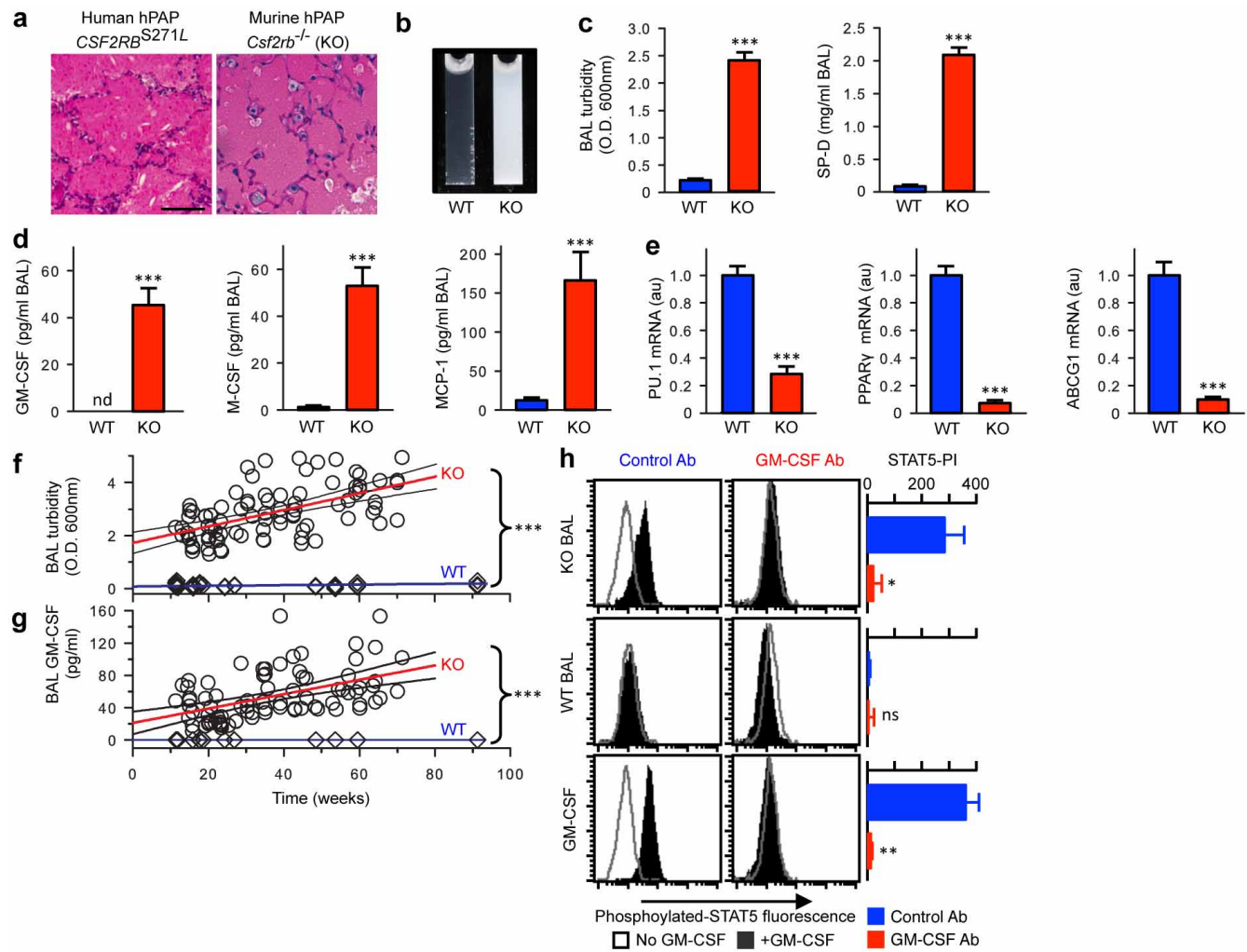
In a second approach, CD45.2⁺ *Csf2rb*^{-/-} mice received PMT of CD45.1⁺ BMDMs and 1 year later, cells isolated from the BAL, blood, bone marrow and spleen were evaluated by flow cytometry to detect CD45.1⁺ cells as a marker for PMT-derived cells.

In a third approach, *Csf2rb*^{-/-} mice received PMT of Lys-M^{GFP} BMDMs and 1 year later, DNA was extracted from the BAL cells (lung), blood leukocytes, bone marrow cells, and spleen using a DNeasy Blood & Tissue Kit (Qiagen). Organ-specific DNA was subjected to PCR amplification using oligonucleotide primers (Extended Data Table 1) specific for the Lys-M^{GFP} knock-in transgene or the unmodified Lysozyme M gene to detect PMT-derived and endogenous cells, respectively, as previously reported²⁵.

A fourth approach was conducted using a specific operating procedure (TSL 6-13) and Good Laboratory Practice (GLP) conditions within the CCHMC Translational Core Laboratory. Here, DNA was extracted from the BAL cells (lung), blood leukocytes, bone marrow cells, and spleen of *Csf2rb*^{-/-} mice that had received PMT of GM-R-GFP-LV *Csf2rb* gene-corrected, *Csf2rb*^{-/-} LSK-derived macrophages 1 year earlier and subjected to quantitative PCR amplification with oligonucleotide primers specific for the R-U5 of GM-R-GFP-LV using Applied Biosystems ABI7900HT Fast Real-Time PCR System (Life Technologies). The number of GM-R-GFP-LV vector copies per microgram of organ-specific DNA was quantified and normalized to the level of mouse apolipoprotein B gene as described previously⁵⁴.

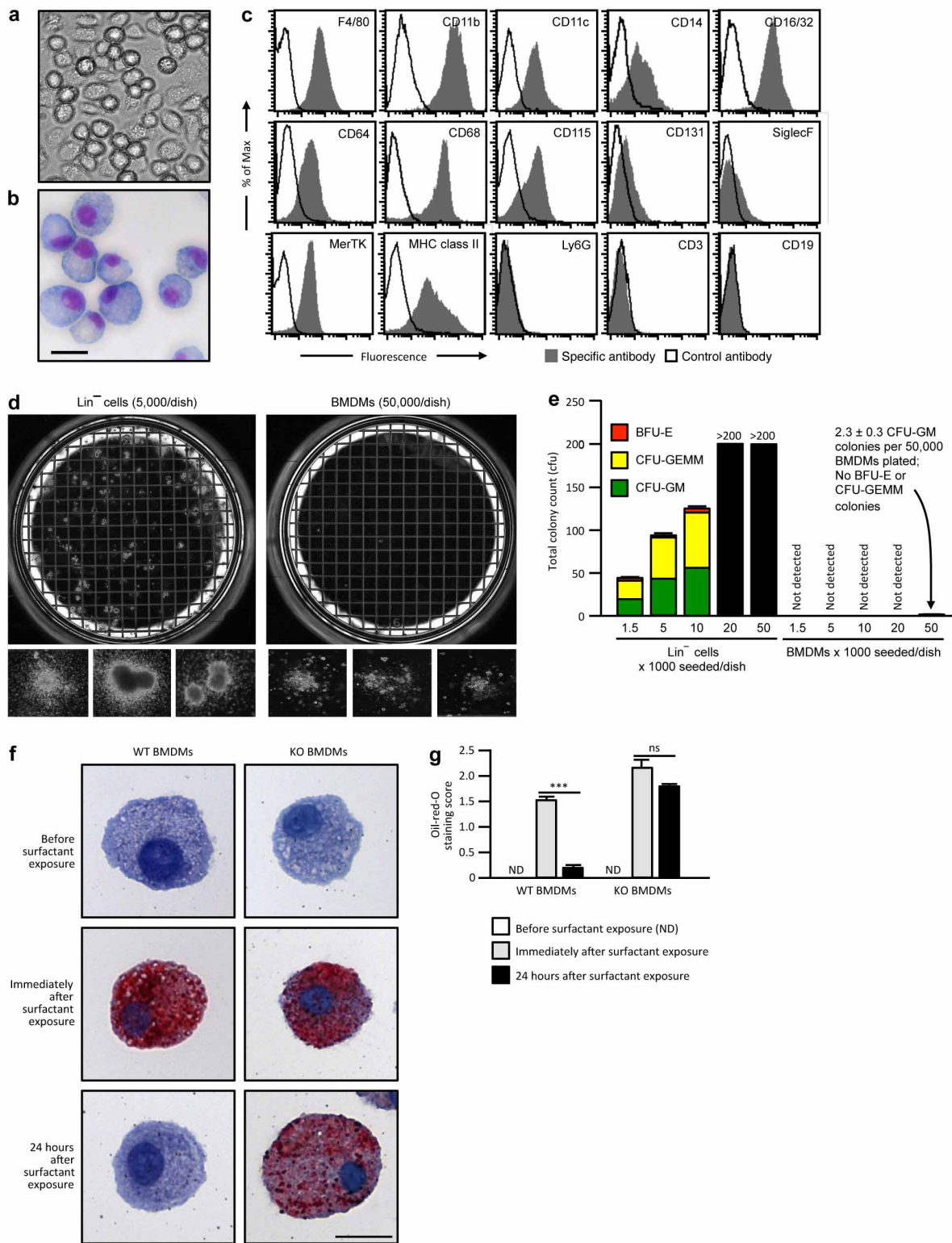
Statistical analysis. Numeric data were evaluated for normality and variance using the Shapiro-Wilk and Levene median tests, respectively, and presented as mean ± s.e.m. (parametric data) or median and interquartile range (nonparametric data). Statistical comparisons were made with Student's *t*-test, one-way analysis of variance, or Kruskal-Wallis rank-sum test as appropriate; post-hoc pairwise multiple comparison procedures were done using the Student-Newman-Keuls or Dunn's method as appropriate. *P* values of ≤0.05 were considered to indicate statistical significance. Based on the use of BAL turbidity (the primary outcome variable for efficacy) measured 2 months after PMT of WT BMDMs into *Csf2rb*^{-/-} mice and compared to age-matched, untreated *Csf2rb*^{-/-} mice, 6 mice per group had a power 0.8 to detect a difference of 1.4 OD 600 nm using a two-tailed Student's *t*-test and a *P* value of 0.05. All studies used male and female mice by randomly assigning mice housed in the same cage to separate experimental groups but without formal randomization or blinding. Results from all mice were included in the final analysis without exclusion. Analyses, including Kaplan-Meyer survival analysis, were performed with SigmaPlot, Version 12.5 (Systat Software, San Jose, CA). All experiments were repeated at least twice, with similar results.

40. Wert, S. E. *et al.* Increased metalloproteinase activity, oxidant production, and emphysema in surfactant protein D gene-inactivated mice. *Proc. Natl Acad. Sci. USA* **97**, 5972–5977 (2000).
41. Sakagami, T. *et al.* Patient-derived granulocyte/macrophage colony-stimulating factor autoantibodies reproduce pulmonary alveolar proteinosis in nonhuman primates. *Am. J. Respir. Crit. Care Med.* **182**, 49–61 (2010).
42. LeVine, A. M., Reed, J. A., Kurak, K. E., Cianciolo, E. & Whitsett, J. A. GM-CSF-deficient mice are susceptible to pulmonary group B streptococcal infection. *J. Clin. Invest.* **103**, 563–569 (1999).
43. Berclaz, P. Y. *et al.* GM-CSF regulates a PU.1-dependent transcriptional program determining the pulmonary response to LPS. *Am. J. Respir. Cell Mol. Biol.* **36**, 114–121 (2007).
44. Perumbeti, A. *et al.* A novel human gamma-globin gene vector for genetic correction of sickle cell anemia in a humanized sickle mouse model: critical determinants for successful correction. *Blood* **114**, 1174–1185 (2009).
45. Kaufman, D. S., Hanson, E. T., Lewis, R. L., Auerbach, R. & Thomson, J. A. Hematopoietic colony-forming cells derived from human embryonic stem cells. *Proc. Natl Acad. Sci. USA* **98**, 10716–10721 (2001).
46. Walters, D. M., Breyssse, P. N. & Wills-Karp, M. Ambient urban Baltimore particulate-induced airway hyperresponsiveness and inflammation in mice. *Am. J. Respir. Crit. Care Med.* **164**, 1438–1443 (2001).
47. Maeda, Y. *et al.* Kras(G12D) and Nkx2-1 haploinsufficiency induce mucinous adenocarcinoma of the lung. *J. Clin. Invest.* **122**, 4388–4400 (2012).
48. Tusher, V. G., Tibshirani, R. & Chu, G. Significance analysis of microarrays applied to the ionizing radiation response. *Proc. Natl Acad. Sci. USA* **98**, 5116–5121 (2001).
49. Benjamini, Y. & Hochberg, Y. Controlling the false discovery rate: a practical and powerful approach to multiple testing. *J. R. Stat. Soc. B* **57**, 289–300 (1995).
50. Richard, E. *et al.* Gene therapy of a mouse model of protoporphyria with a self-inactivating erythroid-specific lentiviral vector without preselection. *Mol. Ther.* **4**, 331–338 (2001).
51. Mizushima, S. & Nagata, S. pEF-BOS, a powerful mammalian expression vector. *Nucleic Acids Res.* **18**, 5322 (1990).
52. Zufferey, R., Donello, J. E., Trono, D. & Hope, T. J. Woodchuck hepatitis virus posttranscriptional regulatory element enhances expression of transgenes delivered by retroviral vectors. *J. Virol.* **73**, 2886–2892 (1999).
53. Arumugam, P. I. *et al.* The 3' region of the chicken hypersensitive site-4 insulator has properties similar to its core and is required for full insulator activity. *PLoS ONE* **4**, e6995 (2009).
54. Arumugam, P. I. *et al.* Improved human β-globin expression from self-inactivating lentiviral vectors carrying the chicken hypersensitive site-4 (chs4) insulator element. *Mol. Ther.* **15**, 1863–1871 (2007).



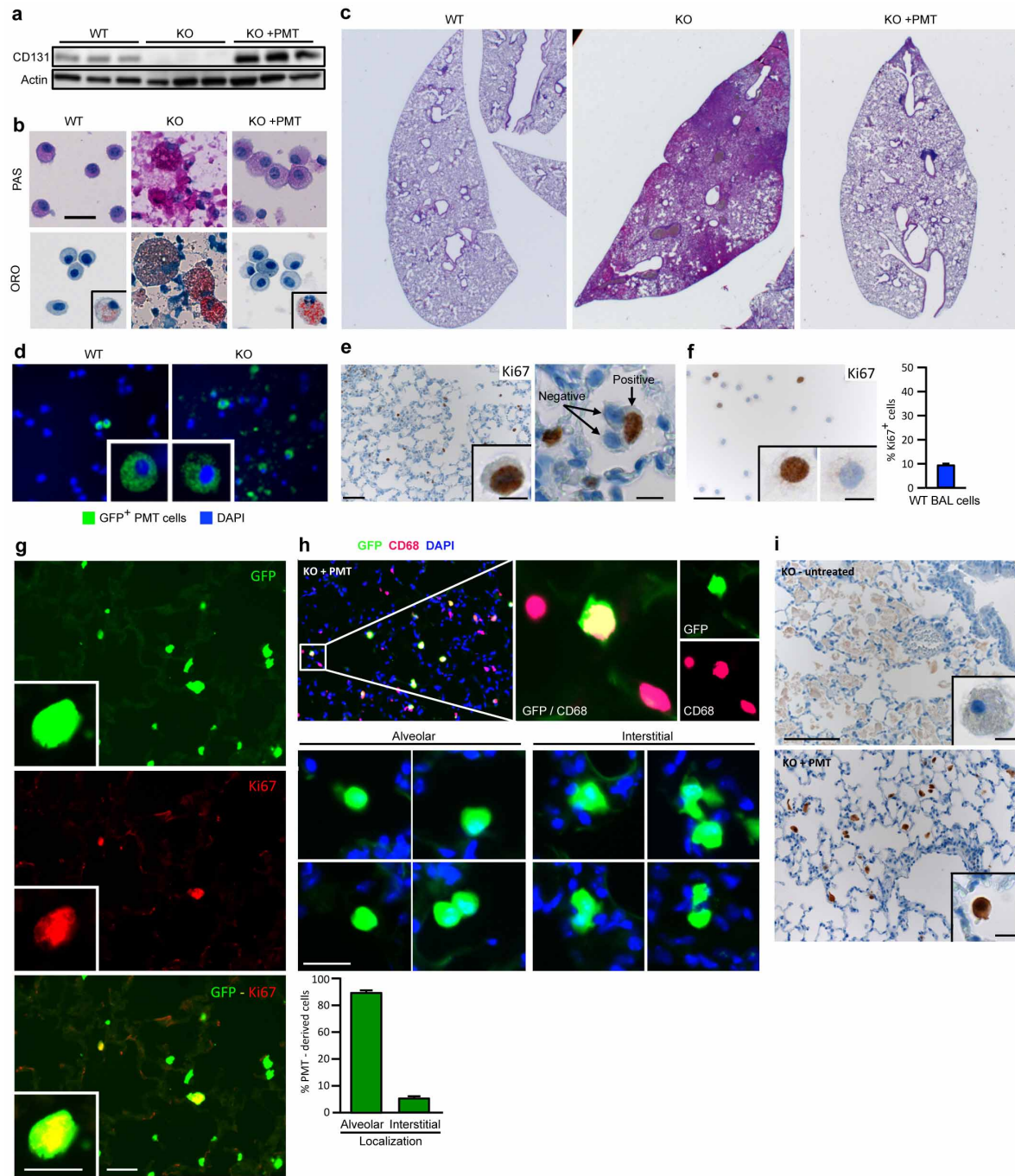
Extended Data Figure 1 | Validation of *Csf2rb^{-/-}* mice as an authentic model of human hPAP. **a**, Typical lung pathology showing surfactant-filled alveoli with well-preserved septa in a child homozygous for *CSF2RB^{S271L}* mutations and identical pulmonary histopathology in a *Csf2rb^{-/-}* mouse. PAS stain. Scale bar, 100 μ m. **b**, Photographs of ‘milky’-appearing BAL from a 14-month-old *Csf2rb^{-/-}* mouse and normal-appearing BAL from an age-matched WT mouse (representative of $n = 6$ mice per group). **c**, Increased BAL turbidity and SP-D concentration in 4-month-old *Csf2rb^{-/-}* mice compared to age-matched WT mice. **d**, BAL fluid biomarkers of hPAP (GM-CSF, M-CSF and MCP-1) are increased in 4-month-old *Csf2rb^{-/-}* mice compared to age-matched WT mice. **e**, Alveolar macrophage biomarkers (*Pu.1*, *Pparg*, *Abcg1* mRNA) are reduced in 4-month-old *Csf2rb^{-/-}* compared to age-matched WT mice. **f**, Progressive increase in BAL turbidity in *Csf2rb^{-/-}*

mice but not age-matched WT mice (linear regression: *Csf2rb^{-/-}*, slope = 0.1271 ± 0.16 (r^2 , 0.311); WT, slope = 0.031 ± 0.005). **g**, Progressive increase in BAL fluid GM-CSF level in *Csf2rb^{-/-}* mice but not age-matched WT mice (linear regression: *Csf2rb^{-/-}*, slope = 0.89 ± 0.016 (r^2 , 0.249); WT, slope = 0). **h**, GM-CSF bioactivity in BAL fluid from 10-month-old *Csf2rb^{-/-}* or WT mice (or 1 ng ml⁻¹ murine GM-CSF) measured in the presence of anti-GM-CSF antibody (GM-CSF Ab) or isotype control (Control Ab) using the GM-CSF-stimulated STAT5 phosphorylation index (STAT5-PI) assay. Data are mean \pm s.e.m. of $n = 7$ mice per group (**c-e**), $n = 4$ (**h**) or symbols representing individual WT ($n = 38$) or *Csf2rb^{-/-}* ($n = 84$) mice and regression fit \pm 95% CI (**f-g**). * $P < 0.05$, ** $P < 0.01$, *** $P < 0.001$. ns, not significant.


Extended Data Figure 2 | Characterization of BMDMs before PMT.

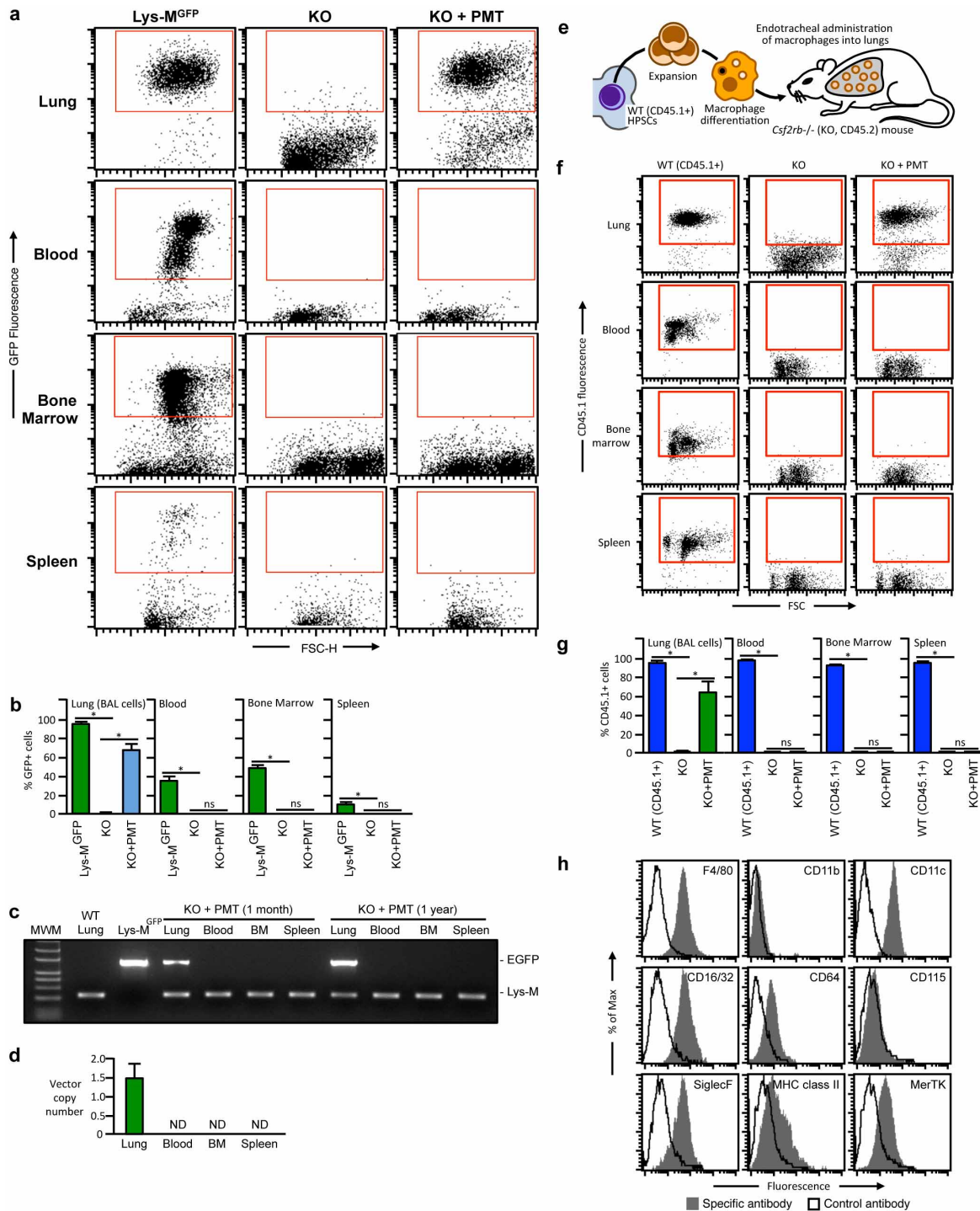
a, b, Photomicrographs of WT BMDMs before transplantation phase-contrast (a) or DiffQuick staining (b) (representative of $n = 7$ BMDM preparations). Scale bar, 20 μ m. **c**, Flow cytometry evaluation of cell-surface phenotypic markers on WT BMDMs before PMT. **d**, Photographs of methylcellulose cultures of Lin⁻ cells (5,000 per dish) from bone marrow (left) and BMDMs (50,000 per dish) prepared as described in the Methods (right) and typical colonies (below) (representative $n = 3$ per condition). **e**, Colony counts of BFU-E, CFU-GEMM and CFU-GM showing that BMDMs contained <0.005% CFU-GM and no BFU-E or CFU-GEMM progenitors, corresponding to 93 CFU-GM per dose of BMDMs administered ($n = 3$

determinations per condition). **f, g**, Evaluation of surfactant clearance capacity. Representative photomicrographs of BMDMs from WT (left) or *Csf2rb*^{-/-} (right) were examined before (top) or immediately after incubation with surfactant for 24 h (middle), or after exposure, removal of extracellular surfactant and culture for 24 h in the absence of surfactant (lower) after oil-red-O staining (representative of $n = 3$ per condition). Scale bar, 20 μ m. **g**, Measurement of surfactant clearance by BMDMs after exposure as just described (f) and quantified using a visual grading scale (the oil-red-O staining index) to measure the degree of staining. Bars represent the mean \pm s.e.m. ($n = 3$ per condition) of oil-red-O staining score for 10 high-power fields for each group. ND, not detected; ns, not significant; *** $P < 0.001$.



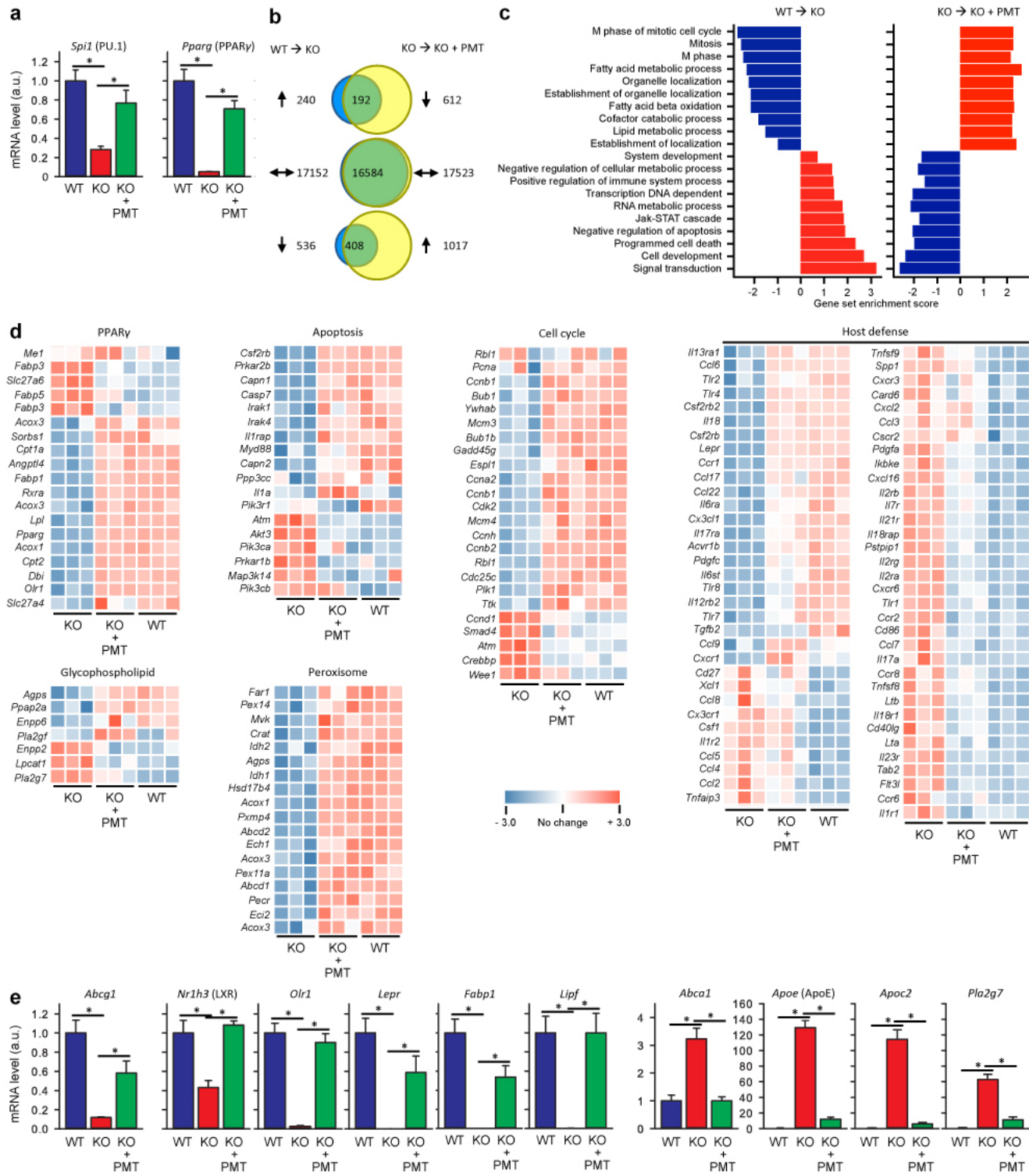
Extended Data Figure 3 | Efficacy of PMT in *Csf2rb*^{-/-} mice and characterization of macrophages after PMT. **a**, Detection of CD131 (top) or actin (bottom) in BAL cells by western blotting 1 year after PMT (each lane represents one mouse of 6 per group). **b**, Representative cytology of BAL obtained 1 year after PMT after staining with PAS or oil red O (ORO) (6 mice per group). Scale bar, 25 μ m. Oil-red-O positive cells were seen rarely in WT mice and occasionally in PMT-treated *Csf2rb*^{-/-} mice (insets). Cytological abnormalities in BAL from untreated *Csf2rb*^{-/-} mice including large, ‘foamy’, PAS- and oil-red-O-stained alveolar macrophages and PAS-stained cellular debris, were corrected by PMT. **c**, Representative photomicrographs of PAS-stained whole-mount lung sections 1 year after PMT. Note that some residual disease remained at 1 year (original magnification, $\times 1$). **d**, GFP⁺ cells in BAL cells from WT or *Csf2rb*^{-/-} mice 2 months after PMT of Lys-M^{GFP} BMDDMs (representative of $n = 3$ (WT) or $n = 6$ (*Csf2rb*^{-/-}) mice) (original magnification, $\times 20$). **e**, Macrophage replication after PMT. *Csf2rb*^{-/-} mice received Lys-M^{GFP} BMDDMs by PMT and paraffin-embedded lung was immunostained for Ki67 1 month or 1 year later. Scale bar, 50 μ m; inset, 10 μ m. **f**, Ki67 staining of BAL cells from untreated WT mice (**e**). Inset shows positive (left) or negative (right) staining. Scale bar, 50 μ m; inset 10 μ m. Graph shows the per cent Ki67⁺ BAL cells in age-matched WT mice ($n = 5$). **g**, Representative immunofluorescence photomicrographs of frozen lung sections 1 year after PMT of Lys-M^{GFP} into *Csf2rb*^{-/-} mice identifying GFP⁺ cells (top), Ki67⁺ cells (middle) and GFP⁺Ki67⁺ (replicating, PMT-derived) cells (bottom) (representative of $n = 3$ mice). Scale bar, 20 μ m; inset scale bar, 10 μ m. Quantitative summary data are shown in Fig. 2c. **h**, Localization of macrophages within the lungs 1 year after PMT of Lys-M^{GFP} BMDDMs into *Csf2rb*^{-/-} mice and visualization in frozen lung sections after CD68 immunostaining, DAPI counter staining, and fluorescence microscopy to detect CD68⁺GFP⁺ cells (that is, PMT-derived macrophages) or CD68⁺GFP⁻ cells (that is, non-PMT-derived endogenous macrophages). Graph shows quantitative data for $n = 6$ mice. **i**, Localization of macrophages in these same mice (**h**) by detecting GFP by immunohistochemical staining of paraffin-embedded lung sections using light microscopy to eliminate potential interference from autofluorescence (representative of $n = 6$ mice). Quantitative summary data are shown in Fig. 3b.

(left) or negative (right) staining. Scale bar, 50 μ m; inset 10 μ m. Graph shows the per cent Ki67⁺ BAL cells in age-matched WT mice ($n = 5$). **g**, Representative immunofluorescence photomicrographs of frozen lung sections 1 year after PMT of Lys-M^{GFP} into *Csf2rb*^{-/-} mice identifying GFP⁺ cells (top), Ki67⁺ cells (middle) and GFP⁺Ki67⁺ (replicating, PMT-derived) cells (bottom) (representative of $n = 3$ mice). Scale bar, 20 μ m; inset scale bar, 10 μ m. Quantitative summary data are shown in Fig. 2c. **h**, Localization of macrophages within the lungs 1 year after PMT of Lys-M^{GFP} BMDDMs into *Csf2rb*^{-/-} mice and visualization in frozen lung sections after CD68 immunostaining, DAPI counter staining, and fluorescence microscopy to detect CD68⁺GFP⁺ cells (that is, PMT-derived macrophages) or CD68⁺GFP⁻ cells (that is, non-PMT-derived endogenous macrophages). Graph shows quantitative data for $n = 6$ mice. **i**, Localization of macrophages in these same mice (**h**) by detecting GFP by immunohistochemical staining of paraffin-embedded lung sections using light microscopy to eliminate potential interference from autofluorescence (representative of $n = 6$ mice). Quantitative summary data are shown in Fig. 3b.



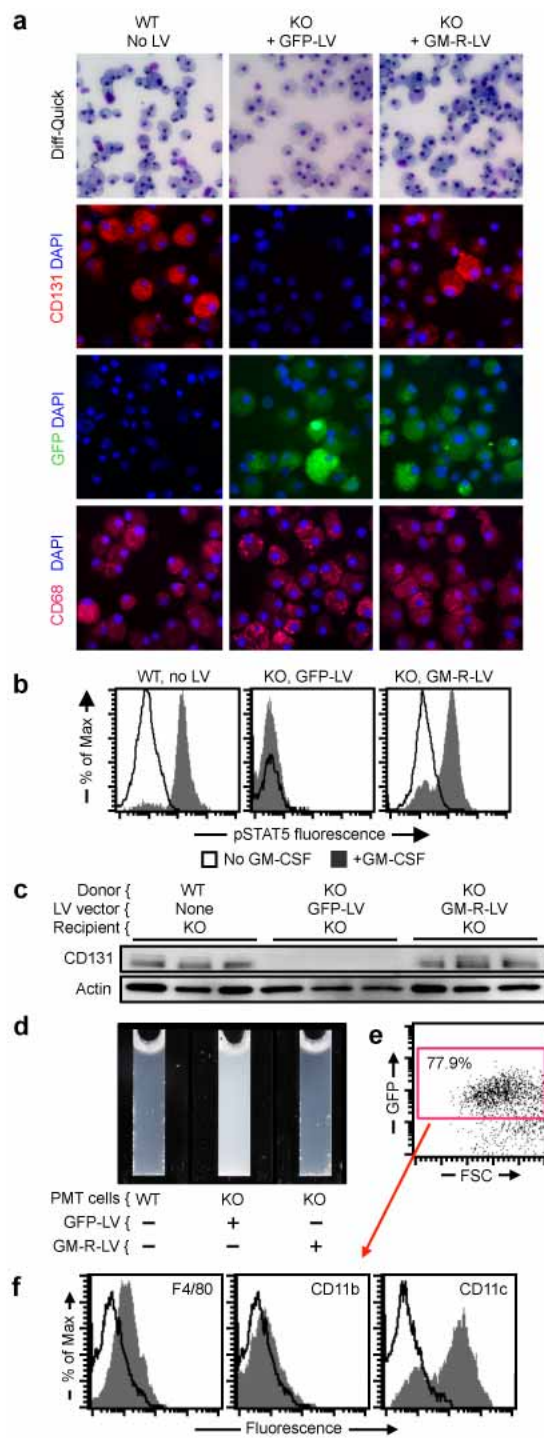
Extended Data Figure 4 | Tissue distribution and characterization of transplanted cells 1 year after PMT. **a–d**, Two-month-old *Csf2rb*^{-/-} mice (4 per group) received one PMT of Lys-M^{GFP} BMDMs. Twelve months later, untreated, age-matched WT Lys-M^{GFP} or *Csf2rb*^{-/-} mice and PMT-treated *Csf2rb*^{-/-} mice were evaluated using flow cytometry to detect GFP⁺ cells in the indicated organs. Representative data (a) and the percentage of GFP⁺ cells in the gated region are shown (b). Similar results were observed in *Csf2rb*^{-/-} mice 2 months after PMT of Lys-M^{GFP} BMDMs except the percentage of GFP⁺ BAL lung cells was not quantified (not shown). **c**, Detection of Lys-M^{GFP} PMT cells by PCR. PCR of genomic DNA from BAL cells (Lung), white blood cells (Blood), bone marrow (BM) cells and splenocytes (Spleen) 1 month or 1 year after Lys-M^{GFP} BMDM PMT was performed to detect EGFP and Lysozyme M gene. BAL cells (Lung) from WT and Lys-M^{GFP} were shown as negative and positive control for EGFP. EGFP was only detected in lung. **d**, Vector copy number analysis after gene-corrected BMDM PMT.

Quantitative PCR with vector-specific primers (R-U5) was performed using genomic DNA from BAL cells (Lung), white blood cells (Blood), bone marrow (BM) cells and splenocytes (Spleen) obtained 1 year after PMT of gene-corrected macrophages. Note that the viral vector was only detected in lung. **e–h**, CD45.2⁺ *Csf2rb*^{-/-} mice received one PMT of CD45.1⁺ BMDMs from congenic WT mice (e) and 1 year later, untreated, age-matched WT (CD45.1⁺) or *Csf2rb*^{-/-} (CD45.2⁺) mice and PMT-treated *Csf2rb*^{-/-} mice were evaluated by flow cytometry to detect CD45.1⁺ cells in the indicated organs. Representative data (f) and the percentage of CD45.1⁺ cells in the gated regions are shown (g). Phenotypic characterization of PMT-derived (CD45.1⁺) cells (as shown in the gated region (f)). Results are similar to those for PMT of Lys-M^{GFP} BMDMs (Fig. 3d). Numeric data are mean \pm s.e.m. of $n = 4$ mice per group (b, d) or $n = 5$ mice per group (g). ND, not detected. * $P < 0.05$. ns, not significant.



Extended Data Figure 5 | Global gene expression analysis of alveolar macrophages from age-matched WT, *Csf2rb*^{-/-} and *Csf2rb*^{-/-} mice 1 year after PMT of WT BMDMs. **a**, Expression of *Spi1* (PU.1) and *Pparg* (PPAR γ) were confirmed by qRT-PCR using independent samples (6 mice per group). **b**, Venn diagrams showing numbers of genes whose expression was altered in alveolar macrophages from *Csf2rb*^{-/-} compared to WT mice (WT → KO) or PMT-treated compared to untreated *Csf2rb*^{-/-} mice (KO → KO + PMT). Only genes with statistically significant changes (false detection rate <10%) of at least twofold were marked as increased (up arrows) or decreased (down arrows). The numbers of genes for which expression was disrupted in *Csf2rb*^{-/-} mice and normalized by PMT (or unchanged in both comparisons) is shown in the overlap regions. **c**, Gene ontology analysis

identifying pathways disrupted in *Csf2rb*^{-/-} mice and restored by PMT. Data show the coordinate increases (red) or decreases (blue) in expression of genes in all gene sets significant at or below a false detection rate of 10% calculated by the Gene Set Test with correction for multiple testing. **d**, Heat maps showing differentially expressed genes in multiple KEGG pathways including PPAR γ -regulated genes, glycophospholipid metabolism, peroxisome function apoptosis, cell cycle control, and immune host defence. Genes with increased or decreased transcript levels are shown by red and blue colours, respectively. **e**, Confirmation by qRT-PCR for selected genes important in lipid metabolism, using independent samples. Data are mean \pm s.e.m. (6 mice per group). * P < 0.05.



Extended Data Figure 6 | Effects of PMT of gene-corrected macrophages on hPAP. **a**, Macrophages derived from *Csf2rb*^{-/-} LSK cells transduced with GM-R-LV or GFP-LV, or from non-transduced WT LSK cells (indicated) were examined by light microscopy after DiffQuick staining (top), or by immunofluorescence microscopy after staining with anti-CD131 (GM-CSF-R-β) and DAPI (upper middle), DAPI alone (lower middle), or anti-CD68 and DAPI (bottom). Images are representative of three experiments per condition. **b**, Evaluation of GM-CSF receptor signalling in the indicated cells (before PMT) by measurement of GM-CSF-stimulated STAT5 phosphorylation by flow cytometry. Representative of $n = 3$ experiments per condition. Quantitative summary data are shown in Fig. 5b. **c**, Western blotting to detect GM-CSF receptor-β (CD131) (top) or actin (bottom, as a loading control) in BAL cells from age-matched *Csf2rb*^{-/-} mice 2 months after PMT as indicated (each lane represents one mouse of $n = 10, 8, 10$ per group, respectively). **d**, Appearance of BAL from age-matched *Csf2rb*^{-/-} mice 2 months after PMT as indicated (representative of $n = 10, 8, 10$ per group, respectively). **e**, **f**, One year after PMT of GM-R-LV transduced *Csf2rb*^{-/-} LSK cell-derived macrophages in *Csf2rb*^{-/-} mice, GFP⁺ cells were identified (**e**) and evaluated for cell surface markers by flow cytometry (**f**) (representative of $n = 7$ mice).

Extended Data Table 1 | Oligonucleotide primers used to quantify mRNA transcripts by qRT-PCR and detection of PMT-derived cellular DNA by PCR

TaqMan® Primers			
Gene name	Accession no.	Product (bp)	Catalogue no.
<i>Spi1</i> (PU.1)	NM_011355.1	91	Mm00488142_m1
<i>Pparg</i>	NM_001127330.1	101	Mm01184322_m1
<i>Abcg1</i>	NM_009593.2	65	Mm00437390_m1
<i>Csf1</i>	NM_001113529.1	70	Mm00432686_m1
<i>Csf2</i>	NM_009969.4	125	Mm01290062_m1
<i>Csf2rb</i>	NM_007780.4	60	Mm00655745_m1
<i>Nr1h3</i> (LXR)	NM_001177730.1	57	Mm00443451_m1
<i>Olr1</i>	NM_138648.2	64	Mm00454586_m1
<i>Lepr</i>	NM_001122899.1	97	Mm00440181_m1
<i>Fabp1</i>	NM_007980.2	116	Mm00433188_m1
<i>Lipf</i>	NM_026334.3	87	Mm00471152_m1
<i>Abca1</i>	NM_013454.3	55	Mm00442646_m1
<i>Apoe</i> (Apo E)	NM_009696.3	64	Mm01307192_m1
<i>Apoc2</i>	NM_009695.3	60	Mm00437571_m1
<i>Pla2g7</i>	NM_013737.5	111	Mm00479105_m1
<i>Gapdh</i>	NM_008084.2	107	4352932E
18S RNA	X03205.1	187	4310893E
Custom Primers			
Gene name	Accession no.	Product (bp)	Sequence (5' → 3')
<i>Lys-M</i> ^{GFP}	NA - transgene	680	aag ctg ttg gga aag gag gg gtc gcc gat ggg ggt gtt ct
Lysozyme-M	M21049	220	aag ctg ttg gga aag gag gg tcg gcc agg ctg act cca ta

Extended Data Table 2 | Effect of the number of macrophages transplanted on the efficacy of PMT therapy of hPAP in *Csf2rb*^{-/-} mice

Parameter	WT	KO	KO + PMT (Macrophages/dose × 10 ⁶)			
			0.5	1	2	4
Turbidity O.D. 600 nm	0.0553 0.023-0.21	1.96 † 1.85-2.74	0.765 ‡ 0.599-0.823	0.685 ‡ 0.472-0.997	0.38 ‡ 0.283-0.685	0.536 ‡ 0.301-0.732
SP-D µg/ml BAL	75.9 51-84	2105 † 1739-2396	1475 ‡ 1367-2034	1414 ‡ 656-1951	911 ‡ 660-1179	1299 ‡ 762-1634
GM-CSF pg/ml BAL	0 0-0	40.8 † 21.4-54.5	28.1 ‡ 15.5-37.8	17.2 ‡ 12.2-20.5	13.8 ‡ 6.97-17.5	14.8 ‡ 10.4-18.0
M-CSF pg/ml BAL	0 0-0	45.0 † 32.3-81.9	30.4 § 14.2-36.0	25.4 § 14.8-36.3	21.7 § 20.1-42.7	29.3 § 23.5-40.5
MCP-1 pg/ml BAL	0.88 0-25.1	135 † 123-163	72.1 ‡ 36.9-121	57.5 ‡ 45.9-80.7	49.0 ‡ 26.1-63.0	64.4 ‡ 28.2-109
<i>Csf2rb</i> mRNA A.U.	1.05 0.86-1.08	0 † 0-0	0.108 ‡ 0.085-0.213	0.167 ‡ 0.095-0.82	0.265 ‡ 0.097-1.46	0.447 ‡ 0.197-0.88
<i>Spi1</i> mRNA A.U.	1.02 0.78-1.13	0.306 † 0.289-0.393	0.468 ‡ 0.27-0.470	0.474 ‡ 0.351-0.707	0.475 ‡ 0.367-0.803	0.480 ‡ 0.446-0.595
<i>Pparg</i> mRNA A.U.	0.929 0.902-1.13	0.052 † 0.0-0.106	0.241 ‡ 0.196-0.362	0.295 ‡ 0.267-0.607	0.516 ‡ 0.327-0.923	0.360 ‡ 0.318-0.603
<i>Abcg1</i> mRNA A.U.	0.933 0.833-1.12	0.08 † 0.07-0.153	0.148 ‡ 0.135-0.183	0.232 ‡ 0.134-0.327	0.179 ‡ 0.106-0.455	0.220 ‡ 0.173-0.229

A.U., arbitrary units; BAL, bronchoalveolar lavage; hPAP, hereditary pulmonary alveolar proteinosis; KO, *Csf2rb* knockout mice; O.D., optical density; PMT, pulmonary macrophage transplantation; WT, wild type.

* Mice received the indicated numbers of WT BMDMs once by PMT. Three months later, BAL fluid and cells were obtained from PMT-treated knockout mice, and age-matched, untreated WT or knockout mice (7 mice per group for each condition evaluated). BAL turbidity, the concentration of SP-D, GM-CSF, M-CSF and MCP-1 in BAL fluid, and the relative abundance of *Csf2rb*, *Spi1* (PU.1), *Pparg* and *Abcg1* mRNA transcripts in alveolar macrophages were measured as described in Methods. All data are presented as median (interquartile range (IQR)) and between-group comparisons were done using non-parametric methods for consistency since results for some groups were either undetectable, not normally distributed or of unequal variance.

† Result is significantly different compared to untreated WT mice (Mann–Whitney rank sum test, $P < 0.001$).

‡ Result is significantly different compared to untreated KO mice (Kruskal–Wallis One Way Analysis of Variance on Ranks with Pairwise comparison to untreated KO mice by the Student–Neuman–Keuls method, $P < 0.05$).

§ Result is not significantly different compared to untreated KO mice (Kruskal–Wallis One Way Analysis of Variance on Ranks, $P = 0.133$).

Extended Data Table 3 | Comparison of the effects of single versus repeated macrophage administrations on the efficacy of PMT therapy of hPAP in *Csf2rb*^{-/-} mice

Parameter	Number of PMT Administrations		P-value †
	One	Four	
Turbidity, O.D. 600 nm	2.014 (1.77-2.53)	1.68 (1.49-3.29)	0.486
SP-D, µg/ml BAL	816 (750-996)	772 (653-796)	0.486
GM-CSF, pg/ml BAL	18.3 (15.3-35.6)	14.3 (13.8-27.8)	0.20
M-CSF, pg/ml BAL	55.5 (50.8-65.6)	29.7 (28.1-49.8)	0.114
MCP-1, pg/ml BAL	88.3 (74.0-118)	53.6 (35.2-78.8)	0.114
<i>Spi1</i> mRNA, A.U.	0.377 (0.284-0.545)	0.322 (0.268-0.362)	0.686
<i>Pparg</i> mRNA, A.U.	0.201 (0.122-0.474)	0.234 (0.169-0.303)	1.0
<i>Abcg1</i> mRNA, A.U.	0.116 (0.098-0.236)	0.117 (0.083-0.131)	0.886

A.U., arbitrary units; BAL, bronchoalveolar lavage; hPAP, hereditary pulmonary alveolar proteinosis; KO, *Csf2rb* knockout mice; O.D., optical density; PMT, pulmonary macrophage transplantation.

* Knockout mice received 2 × 10⁶ macrophages by PMT either once or as four monthly doses. Four months after the initial PMT administration in both groups, BAL fluid and cells were obtained from all mice (6 per group for each condition evaluated). BAL turbidity, the concentration of SP-D, GM-CSF, M-CSF and MCP-1 in BAL fluid, and the relative abundance of *Spi1* (PU.1), *Pparg* and *Abcg1* mRNA transcripts in alveolar macrophages were measured as described in Methods. All data are presented as median (interquartile range (IQR)) and between-group comparisons were done using non-parametric methods for consistency since results for some groups were either not normally distributed or of unequal variance.

† Mann-Whitney Rank Sum Test. P-values of ≤ 0.05 was considered to indicate statistical significance.

Extended Data Table 4 | Effect of PMT of WT or gene-corrected macrophages on haematological indices and lung proinflammatory cytokine levels

Blood Safety Evaluation - PMT Using Wild-Type Macrophages				
Hematologic Parameter	Normal range	WT (n=6)	KO (n=6)	KO + PMT (n=6)
Hemoglobin, g/dL	11.0 – 15.1	12.7 (12.2 – 13.2)	14.5 (13.9 – 15.1) ‡	12.9 (12.2 – 13.4) ¶
Hematocrit, %	35.1 – 45.4	46.5 (44.5 – 47.3)	53.0 (50.2 – 56.3) ‡	47.2 (43.0 – 50.5) ¶
WBC, $\times 10^3/\mu\text{l}$	1.8 – 10.7	2.53 (1.53 – 5.35)	5.08 (3.93 – 6.34) †	3.27 (2.80 – 4.10) ¶
Neutrophils, $\times 10^3/\mu\text{l}$	0.1 – 2.4	0.29 (0.107 – 0.67)	0.89 (0.125 – 2.63) †	0.670 (0.102 – 1.41) §
Lymphocytes, $\times 10^3/\mu\text{l}$	0.9 – 9.3	2.18 (1.06 – 4.26)	3.24 (1.60 – 5.79) †	2.37 (1.76 – 2.94) §
Monocytes, $\times 10^3/\mu\text{l}$	0.0 – 0.4	0.15 (0.11 – 0.24)	0.155 (0.12 – 0.32) †	0.19 (0.15 – 0.25) §
Eosinophils, $\times 10^3/\mu\text{l}$	0.0 – 0.2	0.01 (0.01 – 0.04)	0.02 (0.01 – 0.06) †	0.015 (0.01 – 0.02) §
Basophils, $\times 10^3/\mu\text{l}$	0.0 – 0.2	0.0 (0.0 – 0.01)	0.01 (0.01 – 0.01) †	0.0 (0.0 – 0.003) ¶
Platelets, $\times 10^3/\mu\text{l}$	592 – 2972	558 (463 – 735)	1035 (830 – 1145) ‡	993 (838 – 1031) §
Blood Safety Evaluation - PMT Using Gene-Corrected Macrophages				
Hematologic Parameter	Normal range	WT (n=5)	KO (n=5)	KO + PMT (n=7)
Hemoglobin, g/dL	11.0 – 15.1	10.2 (8.5 – 10.8)	16.9 (13.8 – 18.5) ‡	12.2 (11.1 – 12.9) ¶
Hematocrit, %	35.1 – 45.4	37.5 (33.3 – 40.4)	68.8 (55.4 – 80.3) ‡	49.4 (48.8 – 55.9) ¶
WBC, $\times 10^3/\mu\text{l}$	1.8 – 10.7	1.90 (1.30 – 10.7)	6.48 (5.11 – 8.57) †	5.08 (2.32 – 5.88) §
Neutrophils, $\times 10^3/\mu\text{l}$	0.1 – 2.4	1.31 (0.67 – 8.01)	2.61 (1.71 – 2.85) †	1.49 (0.96 – 2.89) §
Lymphocytes, $\times 10^3/\mu\text{l}$	0.9 – 9.3	0.65 (0.26 – 1.38)	3.39 (2.70 – 5.15) ‡	2.03 (1.15 – 3.33) ¶
Monocytes, $\times 10^3/\mu\text{l}$	0.0 – 0.4	0.25 (0.15 – 0.90)	0.44 (0.29 – 0.87) †	0.25 (0.15 – 0.40) §
Eosinophils, $\times 10^3/\mu\text{l}$	0.0 – 0.2	0.01 (0.01 – 0.43)	0.02 (0.02 – 0.07) †	0.08 (0.01 – 0.16) §
Basophils, $\times 10^3/\mu\text{l}$	0.0 – 0.2	0 (0.0 – 0.07)	0.01 (0.00 – 0.04) †	0.01 (0.00 – 0.03) §
Platelets, $\times 10^3/\mu\text{l}$	592 – 2972	619 (441 – 1478)	1229 (1094 – 1460) †	1381 (872 – 1614) §
Lung Safety Evaluation - PMT Using WT Macrophages				
Cytokine in BAL Fluid		WT (n=6)	KO (n=6)	KO + PMT (n=6)
IL-6, pg/ml		3.01 (1.35 – 3.89)	164 (43.6 – 364) ‡	11.02 (4.87 – 60.1) ¶
IL-1 β , pg/ml		0 (0.0 – 0.0)	3.49 (2.42 – 9.52) ‡	0.92 (0.04 – 1.02) ¶
TNF α , pg/ml		0.52 (0.0 – 0.94)	12.4 (7.22 – 17.9) ‡	2.75 (1.08 – 3.17) ¶
Lung Safety Evaluation - PMT Using Gene Corrected Macrophages				
Cytokine in BAL Fluid		WT (n=5)	KO (n=5)	KO + PMT (n=7)
IL-6, pg/ml		0.30 (0.0 – 2.43)	16.2 (14.1 – 62.1) ‡	29.5 (13.7 – 42.5) §
IL-1 β , pg/ml		0 (0.0 – 0.29)	2.01 (0.47 – 8.1) †	1.65 (0.94 – 3.08) §
TNF α , pg/ml		2.45 (0.46 – 2.76)	6.14 (3.68 – 7.99) ‡	3.06 (2.45 – 7.98) §

BAL, bronchoalveolar lavage; hPAP, hereditary pulmonary alveolar proteinosis; KO, *Csf2rb* knockout mice; O.D., optical density; PMT, pulmonary macrophage transplantation; WT, wild type.

* Knockout mice received WT or *Csf2rb* gene-corrected knockout macrophages (2×10^6 cells per mouse) once by PMT and 12 months later, blood and BAL fluid were obtained from PMT-treated knockout mice, or age-matched, untreated knockout or WT mice and evaluated as described in Methods. Number of mice per group is indicated. All data are presented as median (interquartile range (IQR)) and between-group comparisons were done using non-parametric methods (Mann–Whitney rank sum test) for consistency since results for some groups were either not normally distributed or of unequal variance.

P values ≤ 0.05 were considered to be significant.

† Result is not significantly different compared to WT mice.

‡ Result is significantly different compared to WT mice.

§ Result is not significantly different compared to untreated knockout mice.

¶ Result is significantly different compared to untreated knockout mice.